nature genetics

Recurrent mutations in multiple components of the cohesin complex in myeloid neoplasms

Ayana Kon[1], Lee-Yung Shih[2], Masashi Minamino[3], Masashi Sanada[1,4], Yuichi Shiraishi[5], Yasunobu Nagata[1], Kenichi Yoshida[1], Yusuke Okuno[1], Masashige Bando[3], Ryuichiro Nakato[3], Shumpei Ishikawa[6,7], Aiko Sato-Otsubo[1], Genta Nagae[8], Aiko Nishimoto[6], Claudia Haferlach[9], Daniel Nowak[10], Yusuke Sato[1], Tamara Alpermann[9], Masao Nagasaki[11], Teppei Shimamura[5], Hiroko Tanaka[12], Kenichi Chiba[5], Ryo Yamamoto[13], Tomoyuki Yamaguchi[13,14], Makoto Otsu[15], Naoshi Obara[16], Mamiko Sakata-Yanagimoto[16], Tsuyoshi Nakamaki[17], Ken Ishiyama[18], Florian Nolte[10], Wolf-Karsten Hofmann[10], Shuichi Miyawaki[18], Shigeru Chiba[16], Hiraku Mori[17], Hiromitsu Nakauchi[13,14], H Phillip Koeffler[19,20], Hiroyuki Aburatani[8], Torsten Haferlach[9], Katsuhiko Shirahige[3], Satoru Miyano[5,12] & Seishi Ogawa[1,4]

Cohesin is a multimeric protein complex that is involved in the cohesion of sister chromatids, post-replicative DNA repair and transcriptional regulation. Here we report recurrent mutations and deletions involving multiple components of the cohesin complex, including *STAG2*, *RAD21*, *SMC1A* and *SMC3*, in different myeloid neoplasms. These mutations and deletions were mostly mutually exclusive and occurred in 12.1% (19/157) of acute myeloid leukemia, 8.0% (18/224) of myelodysplastic syndromes, 10.2% (9/88) of chronic myelomonocytic leukemia, 6.3% (4/64) of chronic myelogenous leukemia and 1.3% (1/77) of classical myeloproliferative neoplasms. Cohesin-mutated leukemic cells showed reduced amounts of chromatin-bound cohesin components, suggesting a substantial loss of cohesin binding sites on chromatin. The growth of leukemic cell lines harboring a mutation in *RAD21* (Kasumi-1 cells) or having severely reduced expression of RAD21 and STAG2 (MOLM-13 cells) was suppressed by forced expression of wild-type RAD21 and wild-type RAD21 and STAG2, respectively. These findings suggest a role for compromised cohesin functions in myeloid leukemogenesis.

Recent genetic studies have led to the discovery of a number of new mutational targets in myeloid malignancies, unmasking unexpected roles for deregulated histone modification and DNA methylation in both acute and chronic myeloid neoplasms[1,2]. However, knowledge of the spectrum of gene mutations in myeloid neoplasms remains incomplete. We previously reported a whole-exome sequencing study of 29 paired tumor and normal samples of myeloid neoplasms with myelodysplastic features[3]. Although our major discovery was that frequent spliceosome mutations are uniquely associated with myelodysplasia phenotypes, we also identified hundreds of previously unreported gene mutations[3]. Most of those mutations affected single individuals only and are probably passenger changes. Therefore, their importance in leukemogenesis remains undetermined. However, through closer inspection of an updated list of mutations, including newly validated single-nucleotide variants, we identified additional recurrent mutations involving *STAG2*, a core component of the cohesin complex (Online Methods and **Supplementary Table 1**). In addition, we found that two other functionally related cohesin components, *STAG1* and *PDS5B*, were mutated in single specimens (**Supplementary Fig. 1**).

Cohesin is a multimeric protein complex that is conserved across species and is composed of four core subunits, SMC1, SMC3, RAD21

[1]Cancer Genomics Project, Graduate School of Medicine, The University of Tokyo, Bunkyo-ku, Tokyo, Japan. [2]Division of Hematology-Oncology, Department of Internal Medicine, Chang Gung Memorial Hospital, Chang Gung University, Taipei, Taiwan. [3]Research Center for Epigenetic Disease, Institute of Molecular and Cellular Biosciences, The University of Tokyo, Bunkyo-ku, Tokyo, Japan. [4]Department of Pathology and Tumor Biology, Graduate School of Medicine, Kyoto University, Yoshida-Konoe-cho, Kyoto-shi Sakyo-ku, Kyoto, Japan. [5]Laboratory of DNA Information Analysis, Institute of Medical Science, The University of Tokyo, Minato-ku, Tokyo, Japan. [6]Department of Pathology, The University of Tokyo, Bunkyo-ku, Tokyo, Japan. [7]Department of Genomic Pathology, Medical Research Institute, Tokyo Medical and Dental University, Bunkyo-ku, Tokyo, Japan. [8]Genome Science Division, Research Center for Advanced Science and Technology, The University of Tokyo, Meguro-ku, Tokyo, Japan. [9]Munich Leukemia Laboratory, Munich, Germany. [10]Department of Hematology and Oncology, University Hospital Mannheim, Mannheim, Germany. [11]Division of Biomedical Information Analysis, Department of Integrative Genomics, Tohoku Medical Megabank Organization, Tohoku University, Aoba-ku, Sendai, Japan. [12]Laboratory of Sequence Data Analysis, Human Genome Center, Institute of Medical Science, The University of Tokyo, Minato-ku, Tokyo, Japan. [13]Division of Stem Cell Therapy, Institute of Medical Science, The University of Tokyo, Minato-ku, Tokyo, Japan. [14]Stem Cell and Organ Regeneration Project, Exploratory Research for Advanced Technology (ERATO), Japan Science and Technology Agency (JST), Chiyoda-ku, Tokyo, Japan. [15]Stem Cell Bank, Center for Stem Cell Biology and Regenerative Medicine, Institute of Medical Science, The University of Tokyo, Minato-ku, Tokyo, Japan. [16]Department of Hematology, Faculty of Medicine, University of Tsukuba, Tsukuba, Ibaraki, Japan. [17]Division of Hematology, Department of Medicine, Showa University School of Medicine, Shinagawa-ku, Tokyo, Japan. [18]Division of Hematology, Tokyo Metropolitan Ohtsuka Hospital, Toshima-ku, Tokyo, Japan. [19]Hematology/Oncology, Cedars-Sinai Medical Center, Los Angeles, California, USA. [20]National University of Singapore, Cancer Science Institute of Singapore, Singapore. Correspondence should be addressed to S.O. (sogawa-tky@umin.ac.jp).

Received 15 February; accepted 24 July; published online 18 August 2013; doi:10.1038/ng.2731

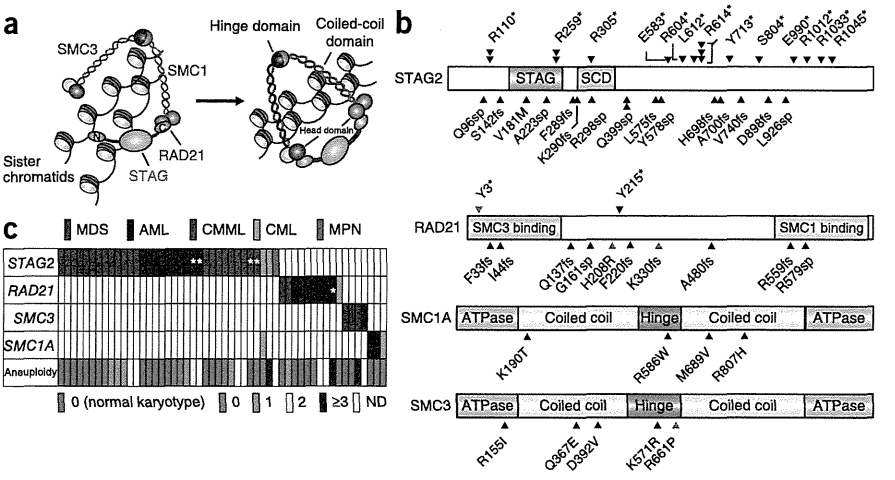

Figure 1 Genetic alterations of the cohesin complex in myeloid neoplasms. (**a**) Cohesin holds chromatin strands within a ring-like structure that is composed of four core components STAG, RAD21, SMC1 and SMC3. (**b**) Mutations in the core components of the cohesin complex found in myeloid malignancies (black arrowheads) and myeloid leukemia-derived cell lines (blue arrowheads). The amino acids in the alterations are referred to using their one-letter abbreviations (for example, R110* represents p.Arg110*). (**c**) Distribution of cohesin mutations and deletions showing a nearly mutually exclusive pattern among different myeloid neoplasms. Gene deletions are indicated by asterisks. The number of numerical chromosome abnormalities in each cohesin-mutated or -deleted case is shown at the bottom. ND, not determined.

and STAG proteins, together with a number of regulatory molecules such as PDS5, NIPBL and ESCO proteins (**Fig. 1a**)[4,5]. Forming a ring-like structure, cohesin is thought to be engaged in the cohesion of sister chromatids during cell division[5], post-replicative DNA repair[6,7] and the regulation of global gene expression through long-range *cis* interactions[8–12]. Germline mutations in cohesin components lead to the congenital multisystem malformation syndromes known as Cornelia de Lange syndrome and Roberts syndrome[13–15].

To investigate a possible role of cohesin mutations in myeloid leukemogenesis, we examined an additional 581 primary specimens of various myeloid neoplasms for mutations in nine cohesin or cohesin-related genes that have been implicated in mitosis[5] using high-throughput sequencing (**Supplementary Table 2**). We also investigated copy-number alterations in cohesin loci in 453 samples using SNP arrays (**Supplementary Table 3**). After excluding known and putative polymorphisms that are registered in the dbSNP or the 1000 Genomes project databases or that were predicted from multiple computational imputations, we identified a total of 60 nonsynonymous mutations involving nine genes in a total of 610 primary samples, which we validated by Sanger sequencing (**Fig. 1b** and **Supplementary Table 4**). After conservative evaluation of the probability of random mutational events across these genes, only four genes remained significantly mutated: *STAG2*, *RAD21*, *SMC1A* and *SMC3* ($P < 0.001$) (**Supplementary Table 5** and Online Methods). In addition, we detected five deletions in *STAG2* ($n = 4$) and *RAD21* ($n = 1$) (**Supplementary Fig. 2a,b** and **Supplementary Table 6**). We also found mutations in these four genes in four of the 34 myeloid leukemia cell lines studied (12%) (**Supplementary Table 7**).

We found mutations and deletions of these four genes in a mostly mutually exclusive manner in a variety of myeloid neoplasms, including acute myeloid leukemia (AML) (19/157), chronic myelomonocytic leukemia (CMML) (9/88), myelodysplastic syndromes (MDS) (18/224) and chronic myelogenous leukemia (CML) (4/64). Mutations were rate in classical myeloproliferative neoplasms (MPN) (1/77) (**Fig. 1c**, **Table 1** and **Supplementary Table 8**). In MDS, mutations were more frequent in refractory cytopenia with multilineage dysplasia and refractory anemia with excess blasts (11.4%) but were rare in refractory anemia, refractory anemia with ring sideroblasts, refractory cytopenia with multilineage dysplasia and ring sideroblasts and MDS with isolated del(5q) (4.2%) ($P = 0.044$). We also evaluated promoter methylation in 33 cases either with ($n = 12$) or without ($n = 21$) cohesin mutations or deletions for which sufficient nonamplified DNA was available using the HumanMethylation450 BeadChip; however, we found no aberrant methylations in cohesin loci, with the exception of hemimethylation of the *SMC1A* promoter that we found in two female cases (**Supplementary Fig. 3**).

We confirmed somatic origins for 17 mutations detected in 16 cases for which matched normal DNA was available (**Supplementary Table 4**). The somatic origins of an additional 23 mutations in *STAG2* or *SMC1A* found in 20 male cases were supported by the presence of reproducible wild-type signals or reads in Sanger and/or deep sequencing of the tumor samples, which were considered to originate from the X chromosome of the residual normal cells (**Supplementary Fig. 4**). In addition, for 20 mutations, the observed allele frequencies determined by pyrosequencing, deep sequencing or digital PCR showed significant deviations from the expected value for polymorphisms in the absence of apparent chromosomal alterations in a SNP array analysis ($P < 0.01$) (**Supplementary Figs. 5** and **6** and **Supplementary Tables 9–12**), suggesting their somatic origins. In addition, 32 of the 33 *STAG2* mutations and all of the nine *RAD21* mutations were either nonsense ($n = 18$), frameshift ($n = 14$) or splice-site ($n = 9$) changes, which were predicted to cause premature truncation of the protein or abnormal exon skipping (**Fig. 1b** and **Supplementary Figs. 7** and **8**). Thus, we considered the majority of the mutations to represent functionally relevant changes, probably of somatic origins (**Supplementary Table 13**).

Most of the cohesin mutations and deletions were heterozygous, except for the *STAG2* and *SMC1A* mutations on the single X chromosome in male cases ($n = 23$). In female samples, the *STAG2* promoter

Table 1 Frequencies of mutations and deletions of cohesin components in 610 myeloid neoplasms

Disease type	*n*	*STAG2*	*RAD21*	*SMC1A*	*SMC3*	Total	Percentage
MDS	224	13	2	0	3	18	8.0
CMML	88	9[a]	0	0	0	9	10.2
AML	157	10	7	2	1	19	12.1
de novo AML	120	8[a]	6	2	1	16	13.3
AML/MRC	37	2[a]	1[a]	0	0	3	8.1
CML	64	2[b]	1	2[b]	0	4	6.3
MPN	77	1	0	0	0	1	1.3
Total	610	35[b]	10	4[b]	4	52	8.5

Diseases are classified according to the World Health Organization 2008 classification. AML/MRC, AML with myelodysplasia-related changes.
[a]Two of the nine cases with *STAG2* alterations in CMML, one of the eight cases with *STAG2* alterations in *de novo* AML, one of the two cases with *STAG2* alterations in AML/MRC cases and one case with *RAD21* alteration in AML/MRC case involved genetic deletions. [b]One CML case having mutations in both *STAG2* and *SMC1A* was counted as a single case. A more detailed list is available in **Supplementary Table 8**.

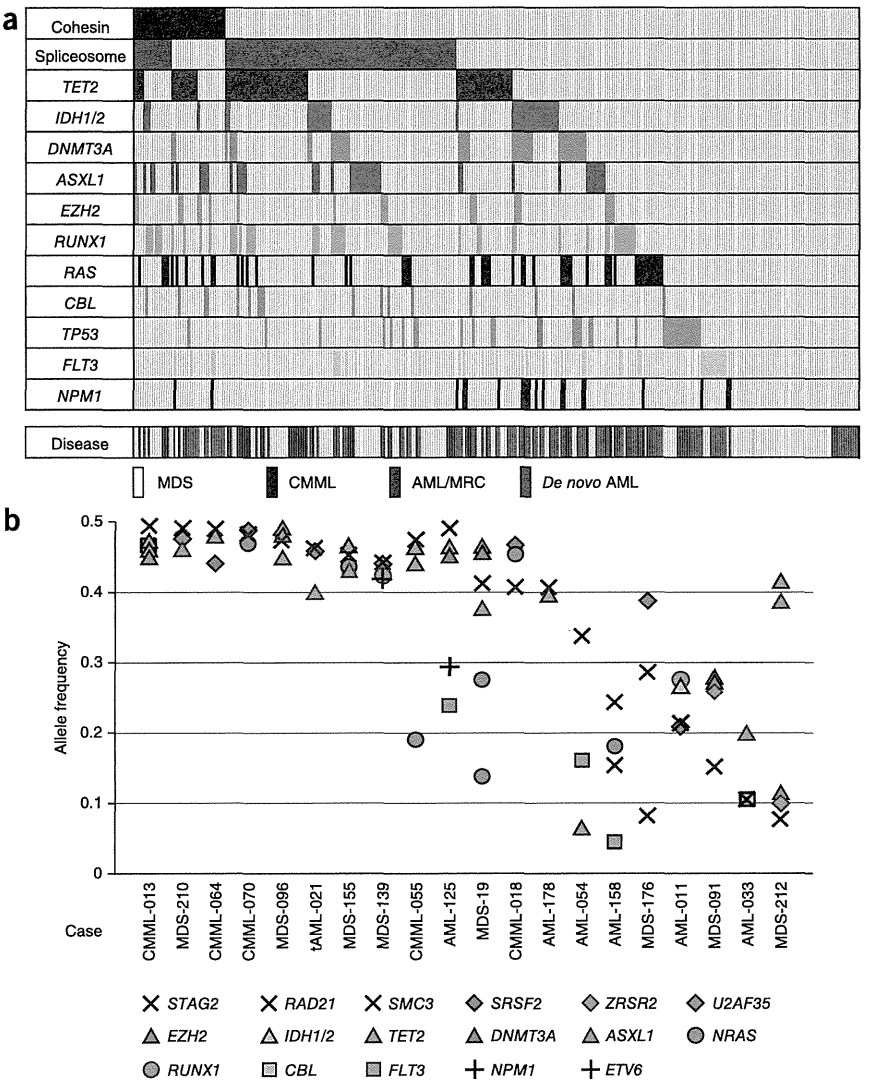

Figure 2 Relationship between cohesin mutations and other common mutations in myeloid malignancies. (**a**) Mutations in the cohesin complex and other common targets in 310 cases with different myeloid neoplasms. The corresponding disease types are shown in the bottom lane. *IDH1/2*, either *IDH1* or *IDH2*. AML/MRC, AML with myelodysplasia-related changes. (**b**) Allele frequencies of mutations in cohesin components and other coexisting mutations in 20 myeloid neoplasms determined by deep sequencing.

was hemimethylated through X inactivation regardless of mutation status (**Supplementary Fig. 3**), and a heterozygous mutation of the unmethylated *STAG2* allele would lead to biallelic *STAG2* inactivation, as has been previously documented in a female case with Ewing's sarcoma[16] and was also confirmed in a single case (CMML-036) in our cohort (**Supplementary Fig. 9**).

Cohesin mutations frequently coexisted with other mutations that are common in myeloid neoplasms and significantly associated with mutations in *TET2* ($P = 0.027$), *ASXL1* ($P = 0.045$) and *EZH2* ($P = 0.011$) (**Fig. 2a**). We performed deep sequencing of the mutant alleles in 20 available samples with cohesin mutations, which allowed for accurate determination of their allele frequencies. The majority of the cohesin mutations (15/20) existed in the major tumor populations, indicating their early origin during leukemogenesis. In the remaining five samples, we found cohesin mutations only in a tumor subpopulation, indicating that the mutations were relatively late events (**Fig. 2b**). Two male cases (MDS-176 and AML-158) harbored two independent subclones with different *STAG2* mutations, indicating that *STAG2* mutation could confer a strong advantage to pre-existing leukemic cells during clonal evolution (**Supplementary Fig. 10**). The number of mutations determined by whole-exome sequencing[3] was significantly higher in four cases with cohesin mutation or deletion compared to cases with no mutation or deletion of cohesin ($P = 0.049$) (**Supplementary Fig. 11**).

Next we investigated the possible impact of mutations on cohesin function. We examined the expression of STAG1, STAG2, RAD21, SMC3, SMC1A and NIPBL in 17 myeloid leukemia cell lines with ($n = 4$) or without ($n = 13$) known cohesin mutations, as well as in the chromatin-bound fractions of 13 cell lines (**Fig. 3a–d** and **Supplementary Table 14**)[14,17–19]. Although we observed an evaluable reduction in RAD21 expression in Kasumi-1 cells that harbored a frameshift alteration in RAD21 (p.Lys330ProfsX6) (**Fig. 3a**), alterations in P31FUJ (RAD21 p.His208Arg), CMY (RAD21 p.Tyr3X) and MOLM-7 (SMC3 p.Arg661Pro) cells were not accompanied by measurable decreases in the corresponding mutated proteins compared to wild-type cell lines. In contrast, we observed severely reduced expression of one or more cohesin components in KG-1 (STAG2)[16] and MOLM-13 (STAG1, STAG2, RAD21 and NIPBL) cells without any accompanying mutations in the relevant genes (**Fig. 3a**). We found no significant differences in protein expression of the cohesin components in cohesin-mutated and non-mutated cell lines in whole-cell extracts (**Fig. 3b**). However, expression of one or more cohesin components, including SMC1, SMC3, RAD21 and STAG2, was significantly reduced in the chromatin-bound fractions of cell lines with mutated or reduced expression of cohesin components, including Kasumi-1, KG-1, P31FUJ, MOLM-7 and MOLM-13 cells, compared with the cell lines with no known cohesin mutations or abnormal cohesin expression ($P < 0.05$), suggesting a substantial loss of cohesin-bound sites on chromatin (**Fig. 3c,d** and **Supplementary Table 14**)[14].

We next examined the effect of forced expression of wild-type cohesin components on the proliferation of a cohesin-mutated cell line (Kasumi-1) or a cell line with reduced expression of cohesin components (MOLM-13). Forced expression of wild-type *RAD21* and/or *STAG2*, but not of a truncated *RAD21* allele, induced significant growth suppression of the Kasumi-1 (with mutated *RAD21*) and MOLM-13 (with severe reduction of RAD21 and STAG2 expression) cell lines but not the K562 and TF1 (with wild-type *RAD21*) cell lines, supporting a leukemogenic role for compromised cohesin functions (**Fig. 4a–c** and **Supplementary Fig. 12a–g**). To explore the effect of forced expression of RAD21 on global gene expression, we performed expression microarray analysis of *RAD21*- and mock-transduced Kasumi-1 cells. In agreement with previous experiments with other cohesin and cohesin-related components, the magnitudes of the

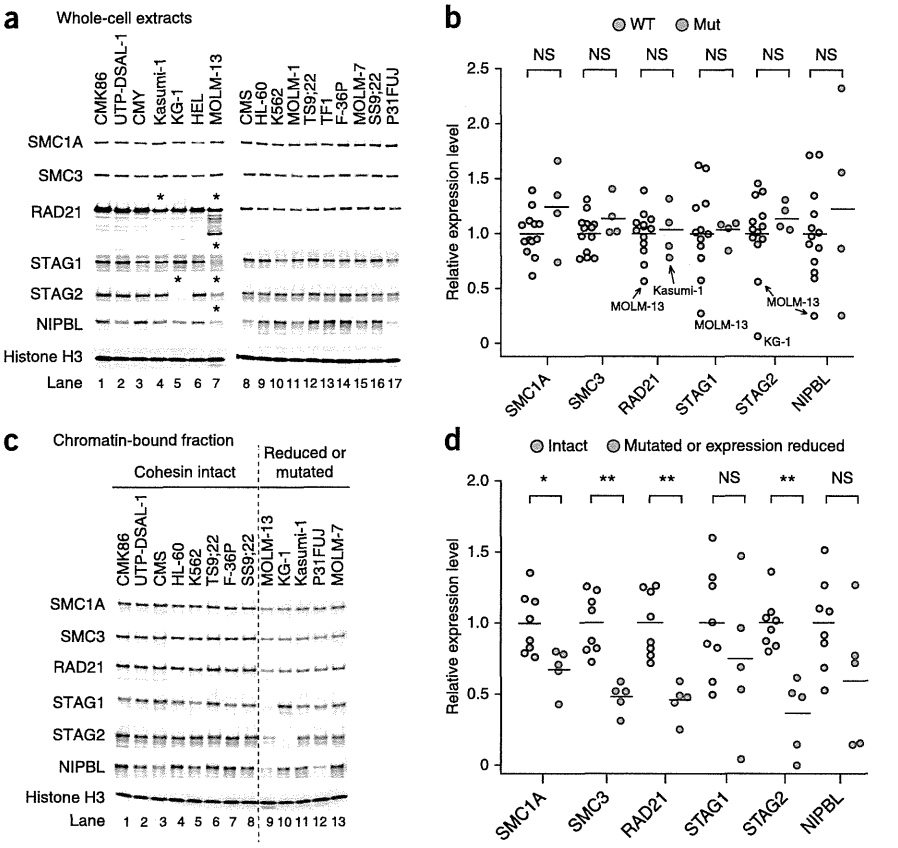

Figure 3 Abnormal cohesin expression and chromatin binding of various cohesin components in myeloid leukemic cell lines. (**a**) Protein blot analysis of the expression of various cohesin components in whole-cell extracts in 17 myeloid leukemia cell lines. Cohesin components showing evaluable reduction in expression are indicated by asterisks, which were reproducible in two independent experiments. (**b**) Expression levels of each cohesin component measured by densitometry after normalization for the mean value across all non-mutated cell lines, with histone H3 signals serving as controls. Evaluably reduced RAD21 expression in Kasumi-1 cells and severely reduced expression of cohesin components in MOLM-13 and KG-1 cells are indicated within the plots. No significant differences (NS) in the expression of the cohesin components were observed between cohesin-mutated and non-mutated cell lines (Mann-Whitney *U* test). Each circle represents a single cell line. (**c**) Protein blot analysis of cohesin components in the chromatin-bound fractions of 13 myeloid leukemia cell lines having intact cohesin (lanes 1–8), cohesin mutations and/or reduced expression of cohesin in whole-cell extracts (lanes 9–13). A representative result of two independent experiments reproducibly showing reduced chromatin-bound cohesin fractions in the cell lines in lanes 9–13 is presented. (**d**) Expression levels of cohesin components in the chromatin-bound fractions measured by densitometry after normalization for the mean value across cell lines with intact cohesin components, with histone H3 signals serving as controls. $*P < 0.05$, $**P < 0.005$ (Mann-Whitney *U* test). Horizontal bars in **b** and **d** indicate the mean values. The densitometric data are presented in **Supplementary Table 14**.

transcriptional changes induced by forced RAD21 expression were generally small[14,16,20]. However, 63 genes reproducibly and significantly showed a more than 1.2-fold increase ($n = 35$) or decrease ($n = 28$) in gene expression ($P < 0.05$), which was validated by quantitative PCR and/or RNA sequencing for 59 of the 63 genes (**Supplementary Fig. 13a–c** and **Supplementary Tables 15** and **16**).

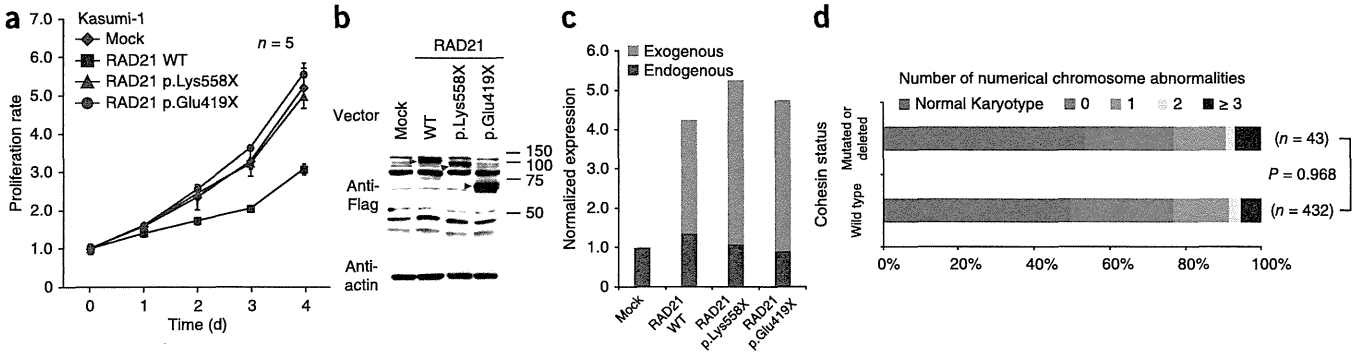

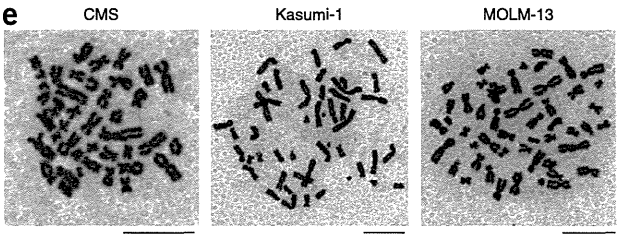

Figure 4 Impact of cohesin mutations on cell proliferation and karyotypes. (**a**) Proliferation of the Kasumi-1 cell line stably transduced with either wild-type RAD21, a truncated allele of *RAD21* (RAD21 p.Lys558X or p.Glu419X) or a mock construct measured by MTT assays ($n = 5$ wells per group). The data are shown as the means ± s.d. of the absorbance at 450 nm relative to the value at day 0. Representative results of three independent experiments are shown. (**b**) Protein blot analysis showing expression of the transduced wild-type and mutant RAD21 alleles. (**c**) Expression of endogenous and exogenous *RAD21* transcripts in Kasumi-1 cells transduced with indicated constructs measured using RNA sequencing by enumerating the corresponding reads. (**d**) The numbers of cases with numerical cytogenetic abnormalities were compared between two groups, those with and those without cohesin mutations or deletions ($P = 0.968$, χ^2). The numbers of numerical chromosome abnormalities are shown at the top. (**e**) Representative metaphases of cell lines with intact (CMS) or abnormal (Kasumi-1 and MOLM-13) cohesin components showing almost normal sister chromatid cohesion. Scale bars, 10 μm.

Mutations in the cohesin complex have recently been reported in a cohort of *de novo* AML and MDS in which four major cohesin components were mutated in 6.0–13.0% of cases[21–25]. Less frequent mutations of cohesin components have been described in other cancers, including *STAG2* mutations in glioblastoma (4/68), melanoma (1/48) and Ewing's sarcoma (1/24)[16]. In primary colon cancer samples, in which impaired cohesion and consequent aneuploidy have been implicated in oncogenesis, mutations in *SMC1A* (4/132), *NIPBL* (4/132), *STAG3* (1/130) and *SMC3* (1/130) have been reported[26]. In contrast, in our cohort of myeloid neoplasms, we found no significant differences in the number of numerical chromosome abnormalities between cohesin-mutated and non-mutated cases, and the 43 cases with cohesin mutations or deletions showed diploid or near-diploid karyotypes, including 23 cases with completely normal karyotypes (**Fig. 4d**). Therefore, in these euploid cases, cohesin-mutated cells were not clonally selected as a result of aneuploidy. Supporting this finding is the observation that expression of *scc1p*, a *RAD21* homolog, at only 13% of its normal level was sufficient for normal cohesion in yeast[27]. Furthermore, Kasumi-1 and MOLM-13 cells showed almost normal cohesion of sister chromatids, even though Kasumi-1 cells have a truncated *RAD21* allele and MOLM-13 cells have substantially reduced expression of multiple cohesin components (**Fig. 4e**).

A growing body of evidence has suggested that cohesin mediates long-range chromosomal *cis* interactions[28] and regulates global gene expression[11,12]. For example, two cohesin subunits, Rad21 and Smc3, have been implicated in the transcriptional regulation of the hematopoietic transcription factor Runx1 in zebrafish[10]. Furthermore, an up to 80% downregulation of *Nipped-B*, a *NIPBL* homolog in *Drosophila*, does not affect chromosomal segregation but does cause impaired regulation of gene expression[20]. We also previously demonstrated that only mild loss (17–28%) of cohesin binding sites within the genome results in deregulated global gene expression[14,18,19]. These observations suggest the possibility that cohesin mutations participate in leukemogenesis through the deregulated expression of genes that are involved in myeloid development and differentiation.

In conclusion, we report frequent mutations in cohesin components that involve a wide variety of myeloid neoplasms. Genetic evidence suggests that aneuploidy may not be the only leukemogenic mechanism, at least *in vivo*, and that deregulated gene expression and/or other mechanisms, such as DNA hypermutability, might also operate in leukemogenesis. Given the integral functions of cohesin for cell viability, genetic defects in cohesin might be potential targets in myeloid neoplasms[14,29].

URLs. dbSNP, http://www.ncbi.nlm.nih.gov/projects/SNP/; the 1000 Genomes Project, http://www.1000genomes.org/; the UCSC Genome Browser; http://genome.ucsc.edu/cgi-bin/hgGateway/; hg19, http://hgdownload.cse.ucsc.edu/goldenPath/hg19/database/; RefSeq genes, http://www.ncbi.nlm.nih.gov/RefSeq/; CNAG/AsCNAR, http://www.genome.umin.jp/; dChip, http://www.dchip.org/; the Integrative Genomics Viewer, http://www.broadinstitute.org/igv/; SIFT, http://sift.jcvi.org/; PolyPhen-2, http://genetics.bwh.harvard.edu/pph2/; Mutation Taster, http://www.mutationtaster.org/.

METHODS

Methods and any associated references are available in the online version of the paper.

Accession codes. Whole-exome sequence data have been deposited in the DNA Data Bank of Japan (DDBJ) repository under accession number DRA000433. RNA sequencing data have been deposited in the DDBJ repository under accession number DRA001013. Microarray data have been deposited in the Gene Expression Omnibus under accession number GSE47684.

Note: Any Supplementary Information and Source Data files are available in the online version of the paper.

ACKNOWLEDGMENTS

This work was supported by Grants-in-Aid from the Ministry of Health, Labor and Welfare of Japan and KAKENHI (23249052, 22134006 and 21790907; S.O.), the Industrial Technology Research Grant Program from the New Energy and Industrial Technology Development Organization (NEDO; S.O.) (08C46598a), NHRI-EX100-10003NI Taiwan (L.-Y.S.), the project for development of innovative research on cancer therapies (p-direct; S.O.) and the Japan Society for the Promotion of Science through the Funding Program for World-Leading Innovative R&D on Science and Technology, initiated by the Council for Science and Technology Policy (CSTP; S.O.). We thank Y. Hayashi (Gunma Children's Medical Centre), R.C. Mulligan (Harvard Medical School), S. Sugano (The University of Tokyo), M. Onodera (National Center for Child Health and Development, Japan) and L. Ström (Karolinska Institute) for providing materials. We thank Y. Yamazaki for cell sorting. We also thank Y. Mori, M. Nakamura, N. Mizota and S. Ichimura for their technical assistance and M. Ueda for encouragement.

AUTHOR CONTRIBUTIONS

A.K., Y.N., K.Y., A.S.-O., Y. Sato and M.S. processed and analyzed genetic materials and performed sequencing and SNP array analysis. Y. Shiraishi, Y.O., R.N., A.S.-O., H.T., T.S., K.C., M.N. and S. Miyano performed bioinformatics analyses of the sequencing data. L.-Y.S. performed pyrosequencing analysis, and A.N. and S.I. performed digital PCR. G.N. and H.A. performed methylation analysis. M.M., M.B. and K.S. performed studies on protein expression of cohesin components. A.K., M.S., T.Y., R.Y., M.O. and H.N. were involved in the functional studies. A.K. and A.S.-O. performed expression microarray experiments and their analyses. L.-Y.S., D.N., T.A., C.H., F.N., W.-K.H., T.H., H.P.K., T.N., H.M., S. Miyawaki, M.S.-Y., K.I., N.O. and S.C. collected specimens and were involved in project planning. A.K., L.-Y.S., M.M., A.S.-O. and S.O. generated figures and tables. S.O. led the entire project, and A.K. and S.O. wrote the manuscript. All authors participated in the discussion and interpretation of the data.

COMPETING FINANCIAL INTERESTS

The authors declare no competing financial interests.

1. Bejar, R., Levine, R. & Ebert, B.L. Unraveling the molecular pathophysiology of myelodysplastic syndromes. *J. Clin. Oncol.* **29**, 504–515 (2011).
2. Marcucci, G., Haferlach, T. & Dohner, H. Molecular genetics of adult acute myeloid leukemia: prognostic and therapeutic implications. *J. Clin. Oncol.* **29**, 475–486 (2011).
3. Yoshida, K. *et al.* Frequent pathway mutations of splicing machinery in myelodysplasia. *Nature* **478**, 64–69 (2011).
4. Gruber, S., Haering, C.H. & Nasmyth, K. Chromosomal cohesin forms a ring. *Cell* **112**, 765–777 (2003).
5. Nasmyth, K. & Haering, C.H. Cohesin: its roles and mechanisms. *Annu. Rev. Genet.* **43**, 525–558 (2009).
6. Ström, L. *et al.* Postreplicative formation of cohesion is required for repair and induced by a single DNA break. *Science* **317**, 242–245 (2007).
7. Watrin, E. & Peters, J.M. The cohesin complex is required for the DNA damage-induced G2/M checkpoint in mammalian cells. *EMBO J.* **28**, 2625–2635 (2009).
8. Dorsett, D. Cohesin, gene expression and development: lessons from *Drosophila*. *Chromosome Res.* **17**, 185–200 (2009).
9. Dorsett, D. *et al.* Effects of sister chromatid cohesion proteins on cut gene expression during wing development in *Drosophila*. *Development* **132**, 4743–4753 (2005).
10. Horsfield, J.A. *et al.* Cohesin-dependent regulation of Runx genes. *Development* **134**, 2639–2649 (2007).
11. Parelho, V. *et al.* Cohesins functionally associate with CTCF on mammalian chromosome arms. *Cell* **132**, 422–433 (2008).
12. Wendt, K.S. *et al.* Cohesin mediates transcriptional insulation by CCCTC-binding factor. *Nature* **451**, 796–801 (2008).
13. Bose, T. & Gerton, J.L. Cohesinopathies, gene expression, and chromatin organization. *J. Cell Biol.* **189**, 201–210 (2010).
14. Deardorff, M.A. *et al.* HDAC8 mutations in Cornelia de Lange syndrome affect the cohesin acetylation cycle. *Nature* **489**, 313–317 (2012).
15. Deardorff, M.A. *et al.* RAD21 mutations cause a human cohesinopathy. *Am. J. Hum. Genet.* **90**, 1014–1027 (2012).

16. Solomon, D.A. *et al.* Mutational inactivation of STAG2 causes aneuploidy in human cancer. *Science* **333**, 1039–1043 (2011).
17. Beckouët, F. *et al.* An Smc3 acetylation cycle is essential for establishment of sister chromatid cohesion. *Mol. Cell* **39**, 689–699 (2010).
18. Liu, J. *et al.* Transcriptional dysregulation in NIPBL and cohesin mutant human cells. *PLoS Biol.* **7**, e1000119 (2009).
19. Liu, J. *et al.* Genome-wide DNA methylation analysis in cohesin mutant human cell lines. *Nucleic Acids Res.* **38**, 5657–5671 (2010).
20. Schaaf, C.A. *et al.* Regulation of the *Drosophila* enhancer of split and invected-engrailed gene complexes by sister chromatid cohesion proteins. *PLoS ONE* **4**, e6202 (2009).
21. Ding, L. *et al.* Clonal evolution in relapsed acute myeloid leukaemia revealed by whole-genome sequencing. *Nature* **481**, 506–510 (2012).
22. Walter, M.J. *et al.* Clonal architecture of secondary acute myeloid leukemia. *N. Engl. J. Med.* **366**, 1090–1098 (2012).
23. Welch, J.S. *et al.* The origin and evolution of mutations in acute myeloid leukemia. *Cell* **150**, 264–278 (2012).
24. The Cancer Genome Atlas Research Network. Genomic and epigenomic landscapes of adult *de novo* acute myeloid leukemia. *N. Engl. J. Med.* **368**, 2059–2074 (2013).
25. Walter, M.J. *et al.* Clonal diversity of recurrently mutated genes in myelodysplastic syndromes. *Leukemia* **27**, 12785–1282 (2013).
26. Barber, T.D. *et al.* Chromatid cohesion defects may underlie chromosome instability in human colorectal cancers. *Proc. Natl. Acad. Sci. USA* **105**, 3443–3448 (2008).
27. Heidinger-Pauli, J.M., Mert, O., Davenport, C., Guacci, V. & Koshland, D. Systematic reduction of cohesin differentially affects chromosome segregation, condensation, and DNA repair. *Curr. Biol.* **20**, 957–963 (2010).
28. Hadjur, S. *et al.* Cohesins form chromosomal *cis*-interactions at the developmentally regulated IFNG locus. *Nature* **460**, 410–413 (2009).
29. Chan, D.A. & Giaccia, A.J. Harnessing synthetic lethal interactions in anticancer drug discovery. *Nat. Rev. Drug Discov.* **10**, 351–364 (2011).

ONLINE METHODS

Patients and samples. Twenty-nine cases analyzed by whole-exome sequencing were described previously[3]. Anonymized genomic DNA from an additional 581 patients with different myeloid neoplasms were collected from collaborating institutes and used for the analyses described below. All the analyses were performed after written informed consent was obtained. This study was approved by the ethics boards of the University of Tokyo, University Hospital Mannheim, University of Tsukuba, the Munich Leukemia Laboratory, Showa University, Tokyo Metropolitan Ohtsuka Hospital and Chang Gung Memorial Hospital.

Cell lines. The CMS, CMY, UTP-DSAL-1, MOLM-1, MOLM-7, HEL, SS9;22 and TS9;22 cell lines were provided by Y. Hayashi. 293gp and 293gpg cells were provided by R.C. Mulligan. P31FUJ and CMK-86 cells were purchased from the Health Science Research Resources Bank (Osaka, Japan). 293T, KG-1, K562 and F-36P cells were obtained from RIKEN BioResource Center Cell Bank (Tsukuba, Japan), and Kasumi-1, HL-60, MOLM-13 and TF-1 cells were from the American Type Culture Collection. Chromosome spreads were performed for the CMS, Kasumi-1 and MOLM-13 cell lines as previously described[14], except that cells were treated with colcemid (100 μg/ml) and hypotonically swollen in 75 mM KCl for 20 min.

Whole-exome sequencing. The whole-exome sequencing of the 29 paired samples of myelodysplasia was previously described[3], through which we identified a total of 497 candidate single-nucleotide variants and insertions/deletions (indels), of which 268 and 167 were determined by Sanger sequencing as true positives and negatives, respectively, with 62 mutations unconfirmed. In the present study, we updated the list of somatic mutations by rigorously validating the remaining 62 unconfirmed mutations by Sanger sequencing and also by deep sequencing (**Supplementary Table 1**).

Mutation analysis of cohesin components. In total, 534 tumor DNA samples from a variety of myeloid neoplasms were analyzed for possible mutations in nine components of the cohesin complex, *STAG1*, *STAG2*, *SMC1A*, *SMC3*, *RAD21*, *PDS5B*, *ESCO1*, *ESCO2* and *NIPBL*, using high-throughput sequencing of pooled exons amplified from pooled genomic DNA samples. In an additional 47 samples, mutations in *STAG2*, *RAD21*, *SMC1A* and *SMC3* were examined by deep sequencing after enrichment for these targets using a SureSelect custom kit (Agilent) designed to capture all of the coding exons from the target genes, performed as previously described with minor modifications in the algorithm for mutation call[30].

For pooled-DNA sequencing, all target exons (n = 232) encompassing 89,323 nucleotides were PCR amplified using a set of primers having common NotI adaptor sequences on their 5′ ends, digested with NotI, ligated using T4 ligase and sonicated to approximately 200-bp fragments using an ultrasonicator (Covaris); these fragments were used for the generation of sequencing libraries according to a modified pair-end protocol from Illumina. The libraries were then sequenced using HiSeq 2000 (Illumina) with a standard 100-bp paired end–reads protocol. On average, 99.5% of the target bases were analyzed at the depth of 12,000 per pool or 1,000 per sample. Data processing and variant calling were performed as previously described[3] with minor modifications. First, each read from a given DNA pool was aligned to the set of target sequences using BLAT[31] with the -fine option. The mapping information in a .psl format was transformed into a .sam format using the my_psl2sam script, which was further converted into the .bam format using SAMtools[32]. Among the successfully mapped reads, reads were removed from further analysis that either mapped to multiple sites, mapped with more than four mismatched bases or had more than ten clipped bases. Next, the Estimation_CRME script was run to eliminate strand-specific errors and exclude PCR-derived errors. Then, a strand-specific mismatch ratio was calculated for each nucleotide variation for both strands using the bases corresponding to 11–50 cycles. By excluding the top five cycles showing the highest mismatch rates, strand-specific mismatch rates were recalculated, and the smaller value between both strands was adopted as the nominal mismatch ratio. In addition, the nucleotide variations that were present across multiple pools were removed based on permutations across different pools using the Permut_Rm_com script because it is probable that such variations result from systemic sequencing errors. Finally, after excluding variations found in the dbSNP database, the database from the 1000 Genomes project or our in-house SNP database, the variants whose mismatch rate exceeded 0.009 were adopted as candidate mutations. Each candidate mutation was validated by Sanger sequencing of the 12 original individual DNAs from the corresponding DNA pools.

The functional impact of each amino acid substitution was evaluated by computer prediction using SIFT[33], PolyPhen-2 (ref. 34) and Mutation Taster[35]. The significance of nonsilent mutations in each cohesin component was evaluated assuming a uniform distribution of the background mutations within the coding regions, which was estimated to be ~0.3 Mb^{-1} on the basis of a previous whole-exome sequencing of myelodysplasia[3].

Determination of variant allele frequencies. Variant allele frequencies were evaluated by deep sequencing of PCR amplicons, pyrosequencing[36,37] and/or digital PCR (Fluidigm CA, US)[38–40] of the variants using nonamplified DNA. For amplicon sequencing, genomic fragments harboring the variants of interest were PCR amplified using NotI-tagged primers. Ninety-two randomly selected SNP loci that do not contain repetitive sequences were amplified using normal genomic DNA as a template, which served as the control. Touch-down PCRs using high-fidelity DNA polymerase KOD-Plus-Neo (TOYOBO, Tokyo) were performed, and an equimolar mixture of all PCR products was prepared for deep sequencing using HiSeq2000 or Miseq (Illumina), as described above, with a 75-bp or 100-bp pair end–read option. To calculate the allele frequency of each variant, all reads were mapped to the target reference sequence using BLAT[31], followed by differential enumeration of the dichotomic variant alleles. For indels, individual reads were first aligned to each of the wild-type and altered sequences and then assigned to the one with better alignment in terms of the number of matched bases.

Array-based copy-number and methylation analyses. Genomic DNA from 453 bone marrow samples with myeloid neoplasms was analyzed using GeneChip SNP genotyping microarrays as previously described using CNAG/AsCNAR software[41,42]. The results of the SNP array karyotyping for 290 of the 453 cases have been previously published[3,41–44]. The promoter methylation of each cohesin component gene was analyzed using the HumanMethylation450 BeadChip (Illumina), as previously described[30,45], in which methylation status was evaluated by calculating the ratio of methylation-specific and demethylation-specific fluorophores (β value) at each CpG site using iScan software (Illumina).

RT-PCR. Complementary DNA synthesis and quantitative RT-PCR analyses were performed as previously described[3]. The primer sequences used are listed in **Supplementary Tables 16** and **17**.

Protein expression of cohesin components in whole-cell extracts and chromatin-enriched fractions. Whole-cell extracts of myeloid cell lines were separated into soluble supernatant and chromatin-containing pellet fractions and analyzed by SDS-PAGE and protein blot analysis for the expression of different cohesin components as previously described[12,14]. Antibodies used for protein blot analysis are described in **Supplementary Table 18**.

Gene expression and cell proliferation assays. A full-length *RAD21* cDNA (BC050381) was provided by S. Sugano. A full-length *STAG2* cDNA was obtained from total cDNA derived from bone marrow cells and cloned into pBluescript. The truncated mutant of *RAD21* was subcloned by PCR. Flag-tagged *RAD21* or *STAG2* cDNAs were constructed into the retrovirus vector pGCDNsamIRESEGFP (provided by M. Onodera)[46] or a tetracycline-inducible lentiviral vector, CS-TRE-Ubc-tTA-IRESPuro. The wild-type *RAD21*, the mutant *RAD21* and/or a mock-induced retroviral vector were generated as previously described[3] and transduced into Kasumi-1, K562 and TF1 cells, which were sorted by GFP marking using a MoFlo FACS cell sorter (Beckman Coulter) or a BD FACSAria cell sorter (BD Biosciences) 48–96 h after retroviral transduction. The wild-type *RAD21*, the wild-type *STAG2* and a mock-induced lentiviral vector were generated as described previously[47], transduced into MOLM-13 cells and selected by 1 μg/ml puromycin. Gene expression was induced by 1 μg/ml doxycycline. For cell growth assays, the cells were inoculated into 96-well culture plates in RPMI 1640 medium supplemented

doi:10.1038/ng.2731

with 5% FCS (and 5 ng/ml GM-CSF for TF1 cells), and cell growth was monitored in three independent experiments by MTT assay using the Cell Counting Kit-8 (Dojindo Co.).

Expression microarray analysis. RNA was extracted from Kasumi-1 cells that were either mock transduced or transduced with wild-type RAD21 and analyzed in triplicate using the Human Genome U133 Plus 2.0 Array (Affymetrix) according to the manufacturer's protocol. For data analysis, raw array signals were first extracted from .CEL files using dChip Software[48]. After background correction and normalization across the six array data sets, the standardized signal value was obtained for each probe set in each of triplicate array experiments, which were compared between mock-transduced and wild-type *RAD21*–transduced cells. Two independent microarray experiments were performed. To identify transcriptionally altered genes, we used the criteria of fold change greater than ±1.2 and $P < 0.05$ (two-tailed paired t test) in two independent experiments.

RNA sequencing. RNA sequencing of *RAD21*-transduced Kasumi-1 cells and subsequent data analyses were performed as previously described[3] with minor modifications. For quantifications of expression values from the RNA sequencing data, we used a slightly modified version of RKPM (reads per kb of exon per million mapped reads) measures[49]. After removing the sequencing reads that were inappropriately aligned or that had low mapping quality, the number of bases on each exonic region for each RefSeq gene[50] was counted. Then the number of bases was normalized per kb of exon and per 100 million aligned bases. Finally, the expression value of each gene was determined by taking the maximum values among the RefSeq genes corresponding to the gene symbol.

We measured RAD21 expression by differentially enumerating endogenous and exogenous *RAD21* sequence reads, which were discriminated by the absence and presence of the Flag sequence, respectively. After normalization by the number of total reads for each sample, the raw differential read counts were further calibrated against the read counts containing the stop codon in *RAD21*.

Statistical analyses. The significance of the difference in frequency of cohesin component mutations between disease subtypes was tested by one-tailed Fisher's exact test. The coexistence of mutations was tested by two-tailed Fisher's direct method. The significance of the difference in the total number of somatic mutations between cohesin-mutated or -deleted and non-mutated or -deleted samples was tested by Mann-Whitney U test. Differences in the number of numerical abnormalities in cytogenetics between two groups with and without cohesin mutations or deletions was assessed by one-sided χ^2 test.

30. Sato, Y. *et al.* Integrated molecular analysis of clear-cell renal cell carcinoma. *Nat. Genet.* doi:10.1038/ng.2699 (24 June 2013).
31. Kent, W.J. BLAT—the BLAST-like alignment tool. *Genome Res.* **12**, 656–664 (2002).
32. Li, H. *et al.* The Sequence Alignment/Map format and SAMtools. *Bioinformatics* **25**, 2078–2079 (2009).
33. Kumar, P., Henikoff, S. & Ng, P.C. Predicting the effects of coding non-synonymous variants on protein function using the SIFT algorithm. *Nat. Protoc.* **4**, 1073–1081 (2009).
34. Adzhubei, I.A. *et al.* A method and server for predicting damaging missense mutations. *Nat. Methods* **7**, 248–249 (2010).
35. Schwarz, J.M., Rodelsperger, C., Schuelke, M. & Seelow, D. MutationTaster evaluates disease-causing potential of sequence alterations. *Nat. Methods* **7**, 575–576 (2010).
36. Ronaghi, M. Pyrosequencing sheds light on DNA sequencing. *Genome Res.* **11**, 3–11 (2001).
37. Shih, L.Y. *et al.* Emerging kinetics of BCR-ABL1 mutations and their effect on disease outcomes in chronic myeloid leukemia patients with imatinib failure. *Leuk. Res.* **37**, 43–49 (2013).
38. Qin, J., Jones, R.C. & Ramakrishnan, R. Studying copy number variations using a nanofluidic platform. *Nucleic Acids Res.* **36**, e116 (2008).
39. Dube, S., Qin, J. & Ramakrishnan, R. Mathematical analysis of copy number variation in a DNA sample using digital PCR on a nanofluidic device. *PLoS ONE* **3**, e2876 (2008).
40. Totoki, Y. *et al.* High-resolution characterization of a hepatocellular carcinoma genome. *Nat. Genet.* **43**, 464–469 (2011).
41. Nannya, Y. *et al.* A robust algorithm for copy number detection using high-density oligonucleotide single nucleotide polymorphism genotyping arrays. *Cancer Res.* **65**, 6071–6079 (2005).
42. Yamamoto, G. *et al.* Highly sensitive method for genomewide detection of allelic composition in nonpaired, primary tumor specimens by use of affymetrix single-nucleotide-polymorphism genotyping microarrays. *Am. J. Hum. Genet.* **81**, 114–126 (2007).
43. Hosoya, N. *et al.* Genomewide screening of DNA copy number changes in chronic myelogenous leukemia with the use of high-resolution array-based comparative genomic hybridization. *Genes Chromosom. Cancer* **45**, 482–494 (2006).
44. Sanada, M. *et al.* Gain-of-function of mutated C-CBL tumour suppressor in myeloid neoplasms. *Nature* **460**, 904–908 (2009).
45. Nagae, G. *et al.* Tissue-specific demethylation in CpG-poor promoters during cellular differentiation. *Hum. Mol. Genet.* **20**, 2710–2721 (2011).
46. Nabekura, T., Otsu, M., Nagasawa, T., Nakauchi, H. & Onodera, M. Potent vaccine therapy with dendritic cells genetically modified by the gene-silencing–resistant retroviral vector GCDNsap. *Mol. Ther.* **13**, 301–309 (2006).
47. Agarwal, S. *et al.* Isolation, characterization, and genetic complementation of a cellular mutant resistant to retroviral infection. *Proc. Natl. Acad. Sci. USA* **103**, 15933–15938 (2006).
48. Li, C. & Wong, W.H. Model-based analysis of oligonucleotide arrays: expression index computation and outlier detection. *Proc. Natl. Acad. Sci. USA* **98**, 31–36 (2001).
49. Mortazavi, A., Williams, B.A., McCue, K., Schaeffer, L. & Wold, B. Mapping and quantifying mammalian transcriptomes by RNA-Seq. *Nat. Methods* **5**, 621–628 (2008).
50. Pruitt, K.D., Tatusova, T., Brown, G.R. & Maglott, D.R. NCBI Reference Sequences (RefSeq): current status, new features and genome annotation policy. *Nucleic Acids Res.* **40**, D130–D135 (2012).

THE ANATOMICAL RECORD 297:111–120 (2014)

Manipulation of Hematopoietic Stem Cells for Regenerative Medicine

YAEKO NAKAJIMA-TAKAGI,[1,2] MITSUJIRO OSAWA,[1,2] AND ATSUSHI IWAMA[1,2]*
[1]Department of Cellular and Molecular Medicine, Graduate School of Medicine, Chiba University, 1-8-1 Inohana, Chuo-ku, Chiba 260-8670, Japan
[2]Japan Science and Technology Corporation, Core Research for Evolutional Science and Technology, Gobancho, Chiyoda-ku, Tokyo, Japan

ABSTRACT

Hematopoietic stem cells (HSCs) are defined by their capacity to self-renew and to differentiate into all blood cell lineages while retaining robust capacity to regenerate hematopoiesis. Based on these characteristics, they are widely used for transplantation and gene therapy. However, the dose of HSCs available for use in treatments is limited. Therefore, extensive work has been undertaken to expand HSCs in culture and to produce HSCs from embryonic stem cells (ESCs) and induced pluripotent stem cells (iPSCs) in order to improve the efficiency and outcome of HSC-based therapies. Various surface markers have been characterized to improve the purification of HSCs and a huge number of cytokines and small-molecule compounds have been screened for use in the expansion of HSCs. In addition, attempts to generate not only HSCs but also mature blood cells from ESCs and iPSCs are currently ongoing. This review covers recent approaches for the purification, expansion or production of human HSCs and provides insight into problems that need to be resolved. Anat Rec, 297:111–120, 2014. © 2013 Wiley Periodicals, Inc.

Key words: hematopoietic stem cells (HSCs); embryonic stem cells (ESCs); induced pluripotent stem cells (iPSCs); regenerative therapy

Blood includes cells of various structures and functions such as oxygen-transporting red blood cells, immunological white blood cells, and hemostasis-mediating platelets. All of these cells are derived from hematopoietic stem cells (HSCs) from various intermediate stages. HSCs are defined as cells possessing the ability to self-renew, in other words, the ability to reproduce themselves, as well as the ability to differentiate into all lineages of blood cells (Morrison et al., 1995, Weissman, 2000). The life of most blood cells is relatively short, and since they are turned-over continuously, HSCs are critical not only for developmental stages but also for maintenance of hematopoietic homeostasis. The dysfunction of HSCs/progenitor cells (PCs) has also been shown to lead to various blood disorders; therefore, HSCs/PCs can serve as therapeutic cellular targets for the treatment of hematological diseases.

One established therapy using HSCs is the HSC transplantation (HSCT). There are currently three different sources of HSCs for HSCT: umbilical cord blood (CB), bone marrow (BM), and mobilized peripheral blood (PB). Each source, however, provides only a limited number of HSCs/PCs. Therefore, advances in technologies such as *ex vivo* culture of HSCs and manipulation of embryonic stem cells (ESCs) and induced pluripotent

Grant sponsor: Grants-in-aid for Scientific Researc on Innovative Areas and for the Global COE Program (Global Center for Education and Research in Immune System Regulation and Treatment), MEXT, Japan; Grant-in-aid for Core Research for Evolutional Science and Technology (CREST) from the Japan Science and Technology Corporation (JST).

*Correspondence to: Atsushi Iwama, M.D. Ph.D., 1–8-1 Inohana, Chuo-ku, Chiba, 260-8670 Japan. Fax: +81-43-226-2191. E-mail: aiwama@faculty.chiba-u.jp

Received 13 September 2013; Accepted 13 September 2013.
DOI 10.1002/ar.22804
Published online 2 December 2013 in Wiley Online Library (wileyonlinelibrary.com).

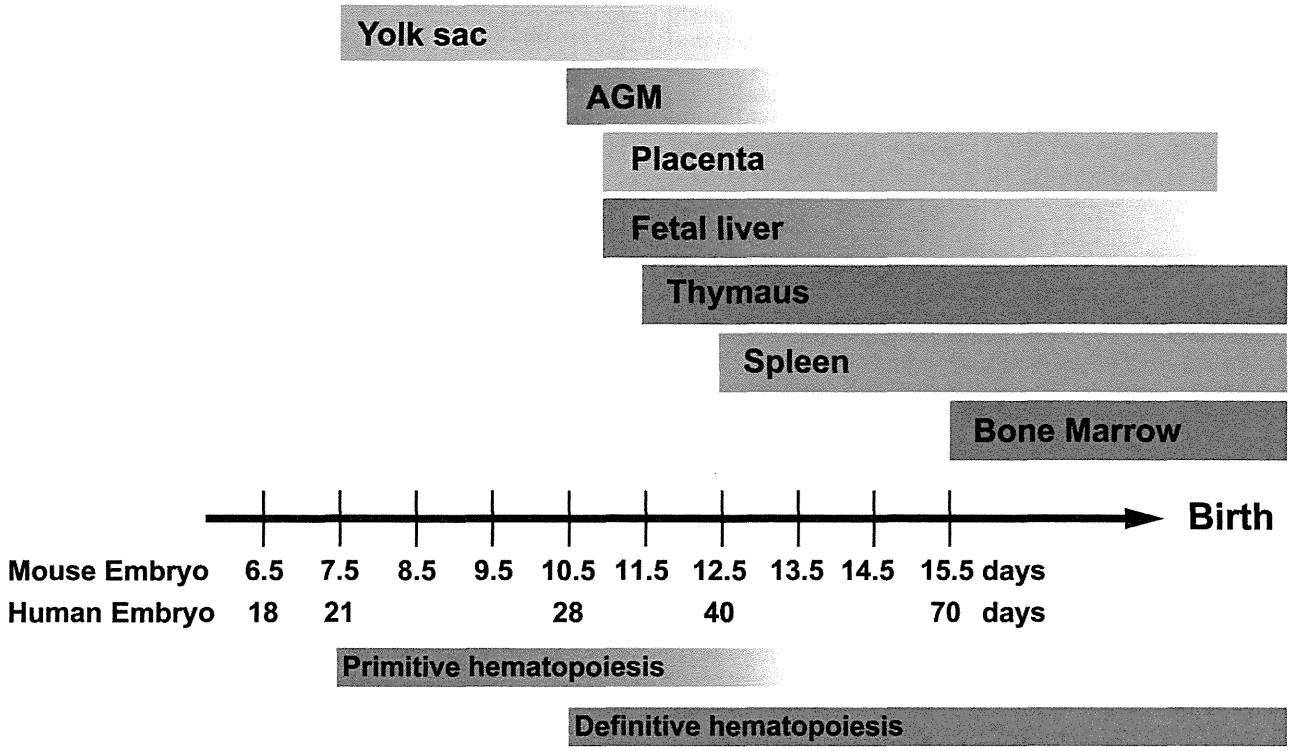

Fig. 1. Hematopoietic organs during mouse and human development. Locations of hematopoiesis during ontogeny. Primitive hematopoiesis is first detected in the yolk sac, and then HSCs arise from the hemogenic endothelium in the ventral aspect of the dorsal aorta in the aorta-gonad-mesonephros (AGM) region, vitelline and umbilical arteries, yolk sac, and placenta. Emerging HSCs migrate first to the fetal liver, and then to the spleen. Eventually, HSCs home to the BM.

stem cells (iPSCs) in order to derive HSCs will have direct benefits on both current and novel therapeutics.

In this article, we review methods to identify HSCs and attempts at *ex vivo* expansion of HSCs/PCs using cytokines, growth factors, niche cells that control the self-renewal, differentiation, and homing of HSCs, small-molecule compounds, and genetic modulation of transcription factors. We also focus on recent approaches to induce HSCs/PCs and mature blood cells from pluripotent stem cells.

DEVELOPMENT OF HSCs

During mammalian development, two waves of hematopoiesis occur in sequential stages: first, a transient wave of primitive hematopoiesis followed by definitive hematopoiesis. These stages are temporally and anatomically distinct, involving unique cellular and molecular regulators. Production of blood cells is started in primitive hematopoiesis that is first detected in the yolk sac as early as embryonic day 7.5 (E7.5) in mice (Palis et al., 1999) (Fig. 1). The first mature blood cells are found closely associated with endothelial cells in the yolk sac structures called blood islands. That hematopoietic and endothelial lineages are produced simultaneously at the same anatomical site led to the hypothesis that these cells are generated from a mesodermal precursor with both endothelial and hematopoietic potential, a cell termed the hemangioblast (Sabin, 1920, Murray, 1932). The extraembryonic yolk sac is considered as the first site of emergence of the hemangioblast. Hemangioblasts differentiate into a hemogenic endothelium intermediate, which gives rise to primitive hematopoietic cells (Lancrin et al., 2009). Primitive hematopoiesis primarily generates nucleated primitive erythrocytes transiently, followed by definitive hematopoiesis which generates all hematopoietic lineages, including enucleated definitive erythrocytes and HSCs with a long-term repopulating activity.

Within the embryo, definitive hematopoiesis takes place in various places (Fig. 1). HSCs emerge directly from a small population of endothelial cells in the conceptus, referred to as "hemogenic endothelium" (Bertrand et al., 2010; Boisset et al., 2010; Kissa et al., 2010). Hemogenic endothelium is located at all sites of HSC emergence, including the ventral aspect of the dorsal aorta in the aorta-gonad-mesonephros (AGM) region, the vitelline and umbilical arteries, the yolk sac, and the placenta. Recently, midgestation embryonic head was also characterized as a site for HSC development (Li et al., 2012). The process by which blood forms from hemogenic endothelium involves an endothelial-to-hematopoietic cell transition during which individual cells bud out and detach from the endothelial layer (Bertrand et al., 2010; Boisset et al., 2010; Kissa et al., 2010). Hemogenic endothelium is distinguished from all other endothelial cells by the presence of a transcription factor called Runx1 (Chen et al., 2009). Runx1 is

expressed in hemogenic endothelial cells, in newly formed hematopoietic cell clusters, and in all functional HSCs (North et al., 1999, 2002). HSCs arising from the hemogenic endothelium migrate first to the fetal liver, and then to the spleen. Eventually, hematopoiesis shifts to the bone marrow (BM), where homeostatic blood formation is maintained throughout life (Wang et al., 2011).

DETECTION AND PURIFICATION OF ADULT HSCs

HSCs reside in a BM niche in a nondividing state from which they occasionally are aroused to undergo cell division on average of once every 1–2 months (Sudo et al., 2000; Foudi et al., 2009). The niche is a specialized anatomic compartment composed of supporting cells and extracellular matrices that are essential for maintaining HSCs/PCs in the BM. Various cell types have been characterized as contributing to the formation of HSC niches, including osteoblasts, endothelial cells, CXCL12 abundant reticular (CAR) cells, mesenchymal progenitor cells, nonmyelinating Schwann cells ensheathing autonomic nerves, macrophages, megakaryocytes, osteoclasts, and so on (Mercier et al., 2011; Wang and Wagers, 2011). The exact contribution of each of these cells to the niche has not been fully elucidated, but recent reports have suggested that these niches are not mutually exclusive in regulating HSC maintenance and mobilization. Although there is the unresolved question of how these complicated niche cells regulate HSCs within the BM, the niche is a source of a variety of signals essential to HSCs/PCs in the form of cytokines, chemokines, growth factors, hormones, cell adhesion proteins, and extracellular–matrix components.

The improvement of technologies using the combination of fluorescence activated cell sorters (FACS) and multistaining procedures with fluorophore-conjugated monoclonal antibodies has remarkably improved the efficiency of the identification and isolation of HSCs. Extensive analyses have been performed to identify the HSC fraction by evaluating the ability of the given fractions to reconstitute the entire hematopoietic system, particularly the three major blood lineages, myeloid cells, T lymphocytes, and B lymphocytes, following transplantation into myeloablated recipients. As a result, mouse HSCs appeared to be highly enriched in the $CD34^{low/-}$c-$Kit^{+}Sca\text{-}1^{+}Lineage\text{-}marker^{-}$ ($CD34^{-}KSL$) cell population, a very rare cell population (0.004% of the mouse BM) with single cell transplantations reconstituting hematopoiesis in more than one out of three recipients (Osawa et al., 1996). The $CD150^{+}CD48^{-}CD41^{-}Lineage\text{-}marker^{-}$ cell population is also highly enriched for HSCs in mice (Kiel et al., 2005).

To evaluate human HSC activity, xenotransplantation systems have been developed using immunodeficient mice such as non-obese diabetic/severe combined immunodeficiency (NOD/SCID) mice, NOD/Shi-scid/IL-$2R\gamma^{null}$ (NOG) mice, and NOD/SCID gamma (NSG) mice (Doulatov et al., 2012). The cells that exhibit long-term reconstitution and differentiation capacity in the immunodeficient mouse are regarded as the closest cells to human HSCs and referred to as SCID-repopulating cells (SRCs). Using these assays, the frequency of SRCs in human CB, BM, and mobilized PB was reported to be

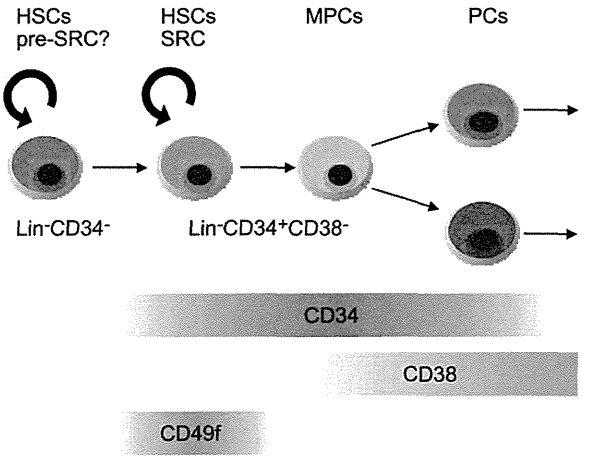

Fig. 2. Surface marker expression profile of human HSCs/PCs. HSCs, Hematopoietic stem cells; MPCs, Multipotent hematopoietic progenitor cells; PCs, Hematopoietic progenitor cells; SRCs, SCID-repopulating cells.

1 in 9.3×10^5, 1 in 3×10^6, and 1 in 6×10^6, respectively (Wang et al., 1997). Among various cell surface markers, the most popular cell surface marker for human HSCs/PCs is CD34 that is expressed on CB and BM cells at a rate of <5% (Krause et al., 1996). Human $CD34^{+}$ cells have been shown to have engraftment potential clinically in numerous autologous and allogeneic transplantation therapies (Vogel et al., 2000). The purification of human HSCs has progressed significantly by examining new antigens along with CD34. The frequency of SRCs in $Lin^{-}CD34^{+}CD38^{-}CD90^{+}CD45RA^{-}$ CB cells is as high as 1 in 10 cells (Majeti et al., 2007) and, notably, Notta et al. succeeded in purifying human HSCs at single-cell resolution in the $Lin^{-}CD34^{+}CD38^{-}CD90^{+}$ $Rho^{lo}CD45RA^{-}CD49f^{+}$ fraction (Notta et al., 2011) (Fig. 2).

ATTEMPTS TO EXPAND HSCs/PCs

The frequency of SRCs in CB is higher compared to those in BM and mobilized PB, but the absolute number of CB cells infused to patients is much lower (Rocha et al., 2004), resulting in higher mortality due to infection, which is most often caused by delayed recovery of neutrophils after transplantation. Thus, efforts to develop techniques for *ex vivo* expansion of CB HSCs/PCs have been underway for the past two decades (Nishino et al., 2012). The ultimate goals of *ex vivo* expansion of CB HSCs/PCs are to increase the number of progenitor cells to establish rapid recovery of neutrophils and platelets, and to augment the number of HSCs in order to increase the chances of life-long hematopoietic reconstitution after transplantation. Various trials have been taken such as liquid culture with cytokines and coculture with stromal cells. However, the clinical trials utilizing these methods have not clearly demonstrated sufficient expansion of HSCs/PCs to overcome the delayed recovery of neutrophils and platelets. To overcome this barrier in HSC/PC expansion, strategies that target signal transduction pathways involved in the self-renewal of HSCs have been exploited by a variety of

TABLE 1. Expansion methods for HSCs from cord blood.

Cytokine	Supplemental factor	Culture period	Amplification efficiency of SRCs	Reference
SCF/TPO/FK3L	IL-6/SIL-6R	7	x4.2	(Ueda et al., 2000)
SCF/TPO/Flt3L/IL-6	TEPA	35	?	(Peled et al., 2004)
SCF/TPO/FK3L/IL-3 or TPO/FK3L	VPA(HDAC inhibitor)	7-21	?	(De Felice et al., 2005)
SCF/TPO/FK3L/IL-3	5azaD+TSA	9	x9.6	(Araki et al., 2006)
SCF/TPO/FK3L/IL-6	DEAB (ALDH inhibitor)	7	x3.4	(Chute et al., 2006)
SCF/TPO/Flt3L/IL-3/IL-6/slL-6R	Delta1	21	x6.0	(Suzuki et al., 2006)
SCF/TPO/FK3L	TEPA	21	?	(da Lima et al., 2008)
SCF/TPO/FGF-1	Angptl-5, IGFBP-2	10	x?20	(Zhang et al., 2008)
SCF/TPO/FK3L/G-CSF	Coculture with MSC	14	?	(Kelly et al., 2009)
SCF/TPO/FK3L	NR-101 (TPOR agonist)	7	x2.9	(Nishino et al., 2009)
SCF/TPO/Flt3L/IL-3/IL-6	Delta 1 $^{ext\text{-}IgG}$	17-21	x6.2	(Delaney et al., 2010)
SCF/TPO/FK3L	Pleiotrophin	7	?	(Himbrug et al., 2010)
SCF/TPO/Flt3L/IL-6	SR1 (AHR antagonist)	14	x17	(Boitano et al., 2011)
	dimethyl PGE2	1 hr	?	(Goessling et al., 2011)
SCF/TPO/Flt3L	BIO (GSK-3|3 inhibitor)	5	x 1	(Ko et al., 2011)
SCF/TPO/Flt3L	Garcinol (HAT inhibitor)	7	x2.5	(Nishino et al., 2011)
SCF/TPO/Flt3L/LDL	SR1 (AHR antagonist)	12	?	(Csaszar et al., 2012)
SCF/TPO/Flt3L/ IL-6	NAM (SIRT1 inhibitor)	21	x8.5	(Peled et al.,2012)

SCF, stem cell factor; TPO, thrombopoietin; Flt3L, FMS-like tyrosine kinase 3 ligand; IL-6, interleukin 6; IL-3, interleukin 3, slL-6R, soluble version of interleukin 6 receptor; FGF-1, fibroblast groeth factor-1; G-CSF, granulocyte colony stimulating factor; LDL, low-density lipoproteins; TEPA, tetraethyl-enepentamine; VPA, valproic acid; HDAC, histone deacetylase; 5azaD, 5-aza-2'-deoxycytidine; TSA, trichostatin A; DEAB, diethylaminobenzalde-hyde; ALDH, aldehyde dehydrogenase; Angptl-5, angiopoietin-like-5; IGFBP-2, insulin growth factor-binding protein-2; MSC, mesenchymal stem cell; TPOR, TPO receptor; AhR, aryl hydrocarbon receptor; PGE2, prostaglandin E2; BIO, 6-bromoindirubin 3'-oxime; GSK-3|3, glycogen synthase kinase-3 beta; HAT, histone acetyltransferase; NAM, Nicotinamide; SIRT1, sirtuin 1

technologies, and a number of protein factors have also been thoroughly screened for the ability to enhance HSC self-renewal during *ex vivo* liquid culture (Table 1). These factors include Angiopoietin-like (ANGPTL)−5, insulin growth factor-binding protein (IGFBP)−2, fibroblast growth factor (FGF)−1 (Zhang et al., 2008), pleiotrophin (Himburg et al., 2010), and Notch ligands (Suzuki et al., 2006; Delaney et al., 2010).

Small-molecule compounds (SMCs) are also attractive tools for HSC/PC expansion (Table 1). Tetraethylenepentamine (TEPA), a copper chelator, enhances the *ex vivo* expansion of HSCs/PCs and is under evaluation in a clinical trial (Peled et al., 2004; de Lima et al., 2008). The 6-bromoindirubin 3′-oxime (BIO), a chemical inhibitor of glycogen synthase kinase-3β (GSK-3β), has been shown to promote the engraftment of cultured $CD34^+$ cells in NOD/SCID mouse (Ko et al., 2011). Valproic acid, a HDAC inhibitor, and Nicotinamide, an inhibitor of the NAD-dependent HDAC sirtuin 1 (SIRT1), have also been reported to promote the expansion of human HSCs *ex vivo* (De Felice et al., 2005; Peled et al., 2012). Among these chemical approaches, one of the most encouraging findings is the discovery of StemRegenin 1 (SR1) that promotes the self-renewal of human HSCs through its antagonizing effect on the aryl hydrocarbon receptor (AHR) (Boitano et al., 2010). $CD34^+$ cells treated with SR1 in the presence of stem cell factor (SCF), thrombopoietin (TPO), Flt3 ligand, and IL-6 for 2 weeks contained >10-fold more short and long term SRCs as compared to uncultured cells or cells cultured with cytokines alone. The positive effect of SR1 on HSC/PC expansion was also confirmed in an automated culture system employing a controlled fed-batch media approach (Csaszar et al., 2012). SR1 has revealed a physiological role for AHR in controlling stemness and also has suggested that signaling molecules downstream of AHR may be promising targets for modulation by SMCs in *ex vivo* HSC/PC expansion.

We have also screened SMCs that are active on HSCs/PCs and identified NR-101, a novel small-molecule c-MPL agonist, as a stimulator of HSC/PC expansion more potent than TPO (Nishino et al., 2009). The signaling by TPO via its receptor, c-MPL or TPOR, plays a crucial role in the maintenance of HSCs. Small-molecule TPOR agonists have recently been shown to be beneficial in the treatment of thrombocytopenia. However, their effects on HSCs have not yet been explored. During a 7-day culture of $CD34^+$ or $CD34^+CD38^-$ HSCs/PCs, NR-101 efficiently promoted the expansion of HSCs/PCs, with a greater than twofold increase compared to culture with TPO. Correspondingly, SRCs were increased 2.9-fold during a 7-day culture with NR-101 compared to freshly isolated $CD34^+$ cells, and 2.3-fold compared to that with TPO. Of note, NR-101 persistently activated STAT5 but not STAT3. Furthermore, NR-101 induced a long-term accumulation of hypoxia-inducible factor-1α (HIF1α) protein and enhanced activation of its downstream target genes. Our findings indicate that SMCs can promote HSC expansion through the modulation of signaling pathways in HSCs. We also identified Garcinol, a plant-derived histone acetyltransferase (HAT) inhibitor, as a novel stimulator of HSC/PC expansion (Nishino et al., 2011). During a 7-day culture of $CD34^+CD38^-$ HSCs/PCs supplemented with Garcinol, numbers of $CD34^+CD38^-$ HSCs/PCs increased more than 4.5-fold compared to controls. Culture with Isogarcinol, a derivative of Garcinol, resulted in a 7.4-fold increase. Furthermore, a 7-day culture of $CD34^+$ HSCs/PCs with Garcinol expanded the number of SRCs 2.5-fold compared to control cells. We also demonstrated

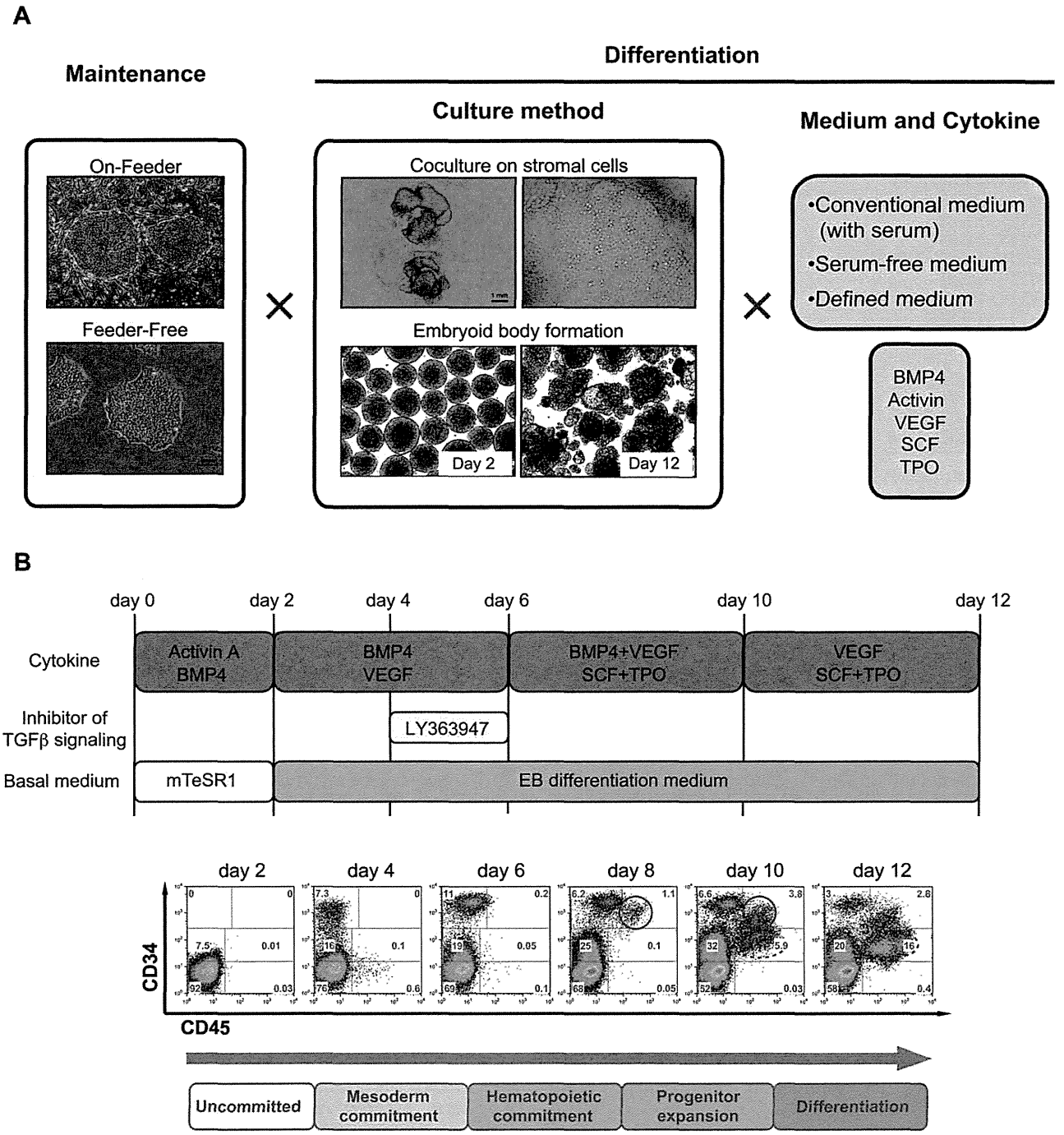

Fig. 3. Hematopoietic differentiation from pluripotent stem cells. (**A**) Schematic representation of the methods used to induce hematopoietic cells from hESCs/iPSCs. Undifferentiated ESCs/iPSCs are maintained on-feeder or in feeder-free culture. Embryoid body (EB) formation and coculture on stromal cells are two major strategies to differentiate hematopoietic cells from ESCs/iPSCs. There are various combinations of medium and cytokines used for differentiation. (**B**) An example of a differentiation protocol using EB culture (Nakajima-Takagi et al., 2013) (upper panel) and flow cytometric profiles of the differentiated hematopoietic cells using this protocol (lower panel). $CD34^{+}CD45^{-}$ endothelial cells (ECs) enriched in hemogenic endothelium give rise to the earliest hematopoietic progenitors, $CD34^{+}CD45^{+}$ hematopoietic progenitor cells (indicated by a circle) and then $CD34^{low}CD45^{+}$ mature hematopoietic cells (indicated by a dotted circle).

that the capacity of Garcinol and its derivatives to expand HSCs/PCs was closely correlated with their inhibitory effects on HATs. Our findings identified Garcinol as the first naturally synthesized product that acts on HSCs/PCs and suggests that the inhibition of HATs could be an alternative approach for manipulating HSCs/PCs. With these evolving technologies to expand HSCs/PCs, the applications of CB cells in

TABLE 2. Attempts to generate repopulating cells from human ESCs.

Expremental system	cell population	Number of transplanted cells	Recipient mice	Transplantation procedure	First tranplantation	Secondary transplantation	Reference
Embryoid Body	$CD45^{neg}PFV$ cells	$5.0x10^5$-$1.7x10^7$	NOD/SCID	i.V.	N.E.	_	(Wang et al., 2005)
		$4.0x10^3$-$1.5x10^4$		IBMT	~0.5%	-	
S17	unsorted cells	$2.0x10^6$-$4.0x10^6$	NOD/SCID	IBMT	0.2-1.4%	0.08-0.4%	(Tian et al., 2006)
S17	$CD34^+Lin^-$ cells	$1.0x10^5$-$1.4x10^5$	Fetal Sheep	i.p.	0.05%	N.E.	(Narayan et al., 2006)
	$CD34^+CD38^-$ cells	$2.6x10^4$-$2.9x10^4$			0.09%	N.E.	
AM20.1B4	unsorted cells	$5.0x10^6$	NOD/SCID/IL2γ^{null}	IBMT	2.5%	_	(Ledran et al., 2008)
UG26.1B6		$5.0x10^6$			1.3%	2.0%	
EL08.1D2		$5.0x10^6$			0.3%	_	
AGM		$5.0x10^6$			2.1%	-	
Fetal liver		$5.0x10^6$			1.0%	-	
Embryoid Body	unsorted cells	$2.0x10^5$	NOD/SCID/IL2Rγ^{null}	IBMT	0.1%	N.E.	(Lu et al., 2009)

S17, mouse bone marrow-derived stromal cell line; AM20.1 B4, stromal cell line generated from the aorta/mesenchyme part of the AGM region of 10 dpc murine embryos; UG26.1 B6, stromal cell line generated from urogenital ridge of the AGM region; EL08.1 D2, stromal cell line generated from the fetal liver of 11 dpc murine embryo; AGM, dorsal Aorta, Gonads, and Mesonephros; i.v., intravenous injection; IBMT, intra-bone marrow transplantation; i.p., intraperitoneal injection; N.E., no engraftment.

transplantation and cell-based therapies is expected to continue to grow.

APPROACHES TO GENERATE HEMATOPOIETIC CELLS FROM HUMAN PLURIPOTENT STEM CELLS

ESCs are pluripotent stem cells derived from the inner cell mass of the blastocyst (Thomson et al., 1998), and iPSCs are ESC-like cells generated by reprogramming somatic cells, most often via forced expression of a combination of transcription factors, such as Oct3/4, Nanog, KLF4, c-Myc, LIN28, and SOX2 (Takahashi et al., 2007, Yu et al., 2007). Human pluripotent stem cells provide a good model for the analysis of the development of human hematopoietic cells and are expected to be a source of numerous hematopoietic cell types for regenerative medicine (Ye et al., 2012). In particular, it is thought that establishment of robust differentiation protocols for various types of blood cells using iPSCs could solve many of the problems of immunological rejection and ethical issues in ESC-based regenerative medicine, and could lead to a cure for various hematological diseases (Togarrati and Suknuntha, 2012). When using hematopoietic cells derived from pluripotent stem cells in regenerative medicine, it is important that the method is safe, efficient, cost-effective, and functional. Extensive trials have been undertaken to efficiently derive HSCs/PCs and mature blood cells from human pluripotent stem cells.

Human ESCs and iPSCs have been demonstrated to reproduce many aspects of embryonic hematopoiesis. Embryoid body (EB) formation (Doetschman et al., 1985) and coculture on stromal feeder cells, such as OP9 (Nakano et al., 1994), S17 (Tian et al., 2006), C3H10T1/2 (Hiroyama et al., 2006), and primary stromal cell lines derived from AGM, fetal liver and fetal BM (Ledran et al., 2008) are two major strategies to induce hematopoietic cells from pluripotent stem cells (Fig. 3). A recent study has provided evidence that hematopoietic differentiation of human ESCs/iPSCs progresses through sequential stages: hemogenic endothelium, then primitive hematopoiesis, and finally definitive hematopoiesis, resembling the development of physiological hematopoiesis (Kaufman, 2009).

Induction of Hematopoietic Stem Cells From Human ESC/iPSCs

It's already been a decade since Kyba et al. first succeeded in generating and expanding HSCs capable of long-term, multilineage reconstitution from mouse ESCs (Kyba et al., 2002). Using a tetracycline-inducible *HoxB4* transgene system, they induced *HoxB4* expression in EBs from days 4–6 of culture. After expansion of *HoxB4*-induced hematopoietic cells on OP9 stromal cells, they transplanted the cells into irradiated syngeneic mice. Recently, it was reported that overexpression of *Lhx2* instead of *HoxB4* also confers a long-term, multilineage reconstituting capacity to ESC/iPSC-derived hematopoietic cells (Kitajima et al., 2011).

Unlike in mice, however, induction of HSCs capable of long-term, multilineage engraftment from human ESCs has yet to be achieved robustly (Table 2). Although overexpression of *HoxB4* promotes the proliferation of hematopoietic cells from human ESCs, it cannot induce

functional HSCs (Wang et al., 2005). Overexpression of a number of genes besides *HoxB4* has been tried, but no success has been achieved so far. Alternative approaches have also have been taken to induce HSCs from human ESCs (Wang et al., 2005; Narayan et al., 2006; Tian et al., 2006; Ledran et al., 2008). Wang and his colleagues succeeded in achieving engraftment of hematopoietic cells induced from hESCs by transplanting $CD45^{neg}$PFV ($CD45^{neg}$PECAM-1^{+}FLK-1^{+}VE-Cadherin^{+}) cells differentiated in EBs directly into the BM of immunodeficient NOD/SCID mice (Wang et al., 2005). However, the level of human chimerism in the BM was remarkably low. So far, Lako's group has had the most success in the derivation of HSCs from hESCs (Ledran et al., 2008). They focused on the microenvironment of hematopoietic development during fetal life, and cocultured human ESC-derived hematopoietic cells on the monolayers of cells derived from mouse AGM or fetal liver, or on the stromal cell lines derived from these embryonic tissues. Among these trials, the human ESC-derived hematopoietic cells cocultured with the AGM-derived stromal cells established about 1.3–2.5% of chimerism in mouse BM. Nevertheless, the engraftment capacity of human ESC-derived hematopoietic cells is remarkably lower than that of CB HSCs. To be able to use ESC/iPSC-derived cells in regenerative medicine, more substantial breakthroughs are needed that are based on the precise understanding of the development of HSCs. We recently showed that SOX17 plays a key role in priming hemogenic potential in endothelial cells, thereby regulating hematopoietic development from hESCs/iPSCs. We further showed that overexpression of *SOX17* in human ESC/iPSC-derived endothelial cells results in expansion of hemogenic endothelium-like cells (Nakajima-Takagi et al., 2013). These accumulating data may help in the development of new technologies.

Induction of Mature Hematopoietic Cells From Human ESC/iPSCs

Erythroid Cells

Red blood cells (RBCs) function to transport oxygen and carbon dioxide through the body, and are the most abundant cells in the blood. For regenerative and transfusion medicine, one of the important points of erythropoiesis from human pluripotent stem cells is globin gene regulation, which changes according to the developmental stages and mediates the function of RBCs. *In vivo*, embryonic-type ξ-and ϵ-globins are expressed in primitive hematopoiesis. In definitive hematopoiesis, these globins switch to fetal-type α- and γ-globins, respectively. Subsequently, γ-globin switches to adult-type β-globin around the time of birth (Peschle et al., 1985).

Recently, several groups described efficient differentiation of human ESCs into RBCs (Chang et al., 2011). In a methylcellulose-based colony-forming cell assay, Kaufman et al. demonstrated that ES-derived erythroid cells expressed α-and β-globin, but did not express fetal γ-globin. No embryonic (ϵ or ξ) globin gene expression was detected, either (Kaufman et al., 2001). But subsequent studies have shown expression of both embryonic and fetal globins by ESC-derived erythroid cells (Cerdan et al., 2004; Qui et al., 2005; Zambidis et al., 2005). For example, Oliver et al. succeeded in large-scale production of RBCs, but the resulting RBCs were similar to primitive erythroid cells present in the yolk sac of early human embryos and did not enucleate. They were fully hemoglobinized and express a mixture of embryonic and fetal globins but no β-globin (Oliver et al., 2006). Eventually, Lu et al. reported a method that induces RBCs with adult β-globin (Lu et al., 2008). RBCs were generated and expanded on a large scale ($1 \times 10^{10}-10^{11}$ cells/six-well plate) from human ESCs via hemangioblasts by a four-step protocol. These cells were oxygen-carrying and showed increased expression of β-globin (from 0% to > 16%), although these cells mainly expressed fetal and embryonic globins. To date, technology in this field has had success in a large scale expansion of RBCs with features of primitive hematopoiesis. However, induction of adult type of RBCs with functional maturity is one issue to resolve in the future.

Megakaryocytes and Platelets

Platelets play an essential role in hemostasis and thrombosis. Platelets are derived from mature multinucleated megakaryocyte (MK) precursors through the cytoplasmic fragmentation and are produced at a rate of 1×10^{11} platelets each day in an adult human. Mature MKs were first differentiated from human ESCs by coculture with OP9 stroma cells in the presence of TPO (Gaur et al., 2006). After 15–17 days of coculture, 20–60% of the floating and loosely adherent cells were $CD41a^{+}CD42b^{+}$, characteristic of megakaryocyte lineage cells. However, no mature functional platelets were detected from these MKs. Subsequent studies reported a differentiation system using coculture with OP9 or C3H10T1/2 stroma cells (Takamaya et al., 2008, 2010). Unique sac-like structures (ES-sac) from the human ESCs/iPSCs appeared on day 14 of culture in the presence of VEGF. Although these ES-sacs included endothelial cells and hematopoietic progenitors, collection of only the hematopoietic progenitors followed by coculture for an additional 7–11days in the presence of TPO, SCF and heparin promoted differentiation into MKs. After culture, 50–60% of cells were $CD41a^{+}CD42a^{+}CD42b^{+}$. Mature MKs from this system can release platelets with morphology and function similar to those isolated from fresh plasma. Lu et al. demonstrated a platelet generation system under serum-and feeder-free conditions using hemangioblasts/blast cells as intermediates (Lu et al., 2011). They demonstrated an efficient method for the differentiation of human ESCs into MKs, and that the platelets subsequently generated are functionally similar to normal blood platelets *in vitro* as well as in living animals. Because platelets contain no genetic material, they are ideal candidates for early clinical translation involving human pluripotent stem cells.

B Cells and T Cells

B cell lineage differentiation has been achieved by sequential exposure of human ESCs to OP9 and MS5 stromal cells (Vodyanik et al., 2005). $CD34^{+}$ cells derived from coculture with OP9 stromal cells were further cultured on MS5 stromal cells in the presence of SCF, Flt3-L, IL-7, and IL-3, and differentiated into lymphoid (B and natural killer cells) as well as myeloid (macrophages and granulocytes) lineages. Using similar protocol, pre-B cells that exhibit multiple genomic D-JH

rearrangements were induced from human iPSCs (Carpenter et al., 2011).

Galic et al. demonstrated that human ESCs could differentiate into the T lymphoid lineage, expressing CD4, CD8, CD3, CD7, and CD1a, for the first time by coculture with OP9 cells followed by engraftment into human thymic tissues in SCID-hu (thy/Liv) mice (Galic et al., 2006), a humanized mouse model constructed by insertion of small pieces of human fetal liver and thymus under the renal capsule of severe combined immunodeficient (SCID) mice (McCune et al., 1988, Namikawa et al., 1990). The same group showed that T cell progenitors could be derived from human ESCs cultured as EBs (Galic et al., 2009).

Differentiation systems using OP9 cells that ectopically express the Notch ligand Delta-like 1 (DL1) has been used very effectively to analyze the T-lineage potential. Timmermans et al. showed that human ESC also could generate T cells via a differentiation system using OP9-DL1 cells (Timmermans et al., 2009). When hematopoietic zones (HZs) formed from human ESCs on normal OP9 feeders, they were transferred to OP9-DL1 feeders and cultured in the presence of Flt-3L, IL7, and SCF. The cells expanded and differentiated into T cells, which displayed both the TCR$\alpha\beta$ and TCR$\gamma\delta$ phenotypes and proliferated and secreted cytokines in response to mitogens.

CONCLUSIONS

Although remarkable progress has been made in the purification of HSCs/PCs and techniques for the expansion of HSCs/PCs, further efforts are still required in order to assure the efficacy and safety of expanded HSCs for transplantation and cell-based therapies. Generation of HSCs and mature hematopoietic cells from human ESCs and iPSCs also requires more technical breakthroughs in order to apply these approaches to clinical therapies. To overcome these problems, it is necessary to keep trying to elucidate the pathways fundamentally supporting the development, maintenance, and differentiation of HSCs and to assess the suitability of these pathways for practical manipulation of HSCs. Improvement in the systems we use to evaluate human HSCs in immunodeficient mice will be also important in making pre-clinical assessments. It is especially desirable to improve the engraftment rate of human HSCs/PCs. With these evolving technologies to expand and produce HSCs, the manipulation of HSCs will secure its place as an instrumental tool in transplantation and cell-based therapies.

ACKNOWLEDGEMENTS

The authors thank George Wendt for critical reading of the manuscript.

LITERATURE CITED

Araki H, Mahmud N, Milhem M, Nunez R, Xu M, Beam CA, Hoffman R. 2006. Expansion of human umbilical cord blood SCID-repopulating cells using chromatin-modifying agents. Exp Hematol 34:140–149.

Bertrand JY, Chi NC, Santoso B, Teng S, Stainier DY, Traver D. 2010. Haematopoietic stem cells derive directly from aortic endothelium during development. Nature 464:108–111.

Boisset JC, van Cappellen W, Andrieu-Soler C, Galjart N, Dzierzak E, Robin C. 2010. *In vivo* imaging of haematopoietic cells emerging from the mouse aortic endothelium. Nature 464:116–120.

Boitano AE, Wang J, Romeo R, Bouchez LC, Parker AE, Sutton SE, Walker JR, Flaveny CA, Perdew GH, Denison MS, Schultz PG, Cooke MP. 2010. Aryl hydrocarbon receptor antagonists promote the expansion of human hematopoietic stem cells. Science 329: 1345–1348.

Carpenter L, Malladi R, Yang CT, French A, Pilkington KJ, Forsey RW, Sloane-Stanley J, Silk KM, Davies TJ, Fairchild PJ, Enver T, Watt SM. 2011. Human induced pluripotent stem cells are capable of B-cell lymphopoiesis. Blood 117:4008–4011.

Cerdan C, Rouleau A, Bhatia M. 2004. VEGF-A165 augments erythropoietic development from human embryonic stem cells. Blood 103:2504–2512.

Chang KH, Bonig H, Papayannopoulou T. 2011. Generation and characterization of erythroid cells from human embryonic stem cells and induced pluripotent stem cells: an overview. Stem Cells Int 2011:791604.

Chen MJ, Yokomizo T, Zeigler BM, Dzierzak E, Speck NA. 2009. Runx1 is required for the endothelial to haematopoietic cell transition but not thereafter. Nature 457:887–891.

Chute JP, Muramoto GG, Whitesides J, Colvin M, Safi R, Chao NJ, McDonnell DP. 2006. Inhibition of aldehyde dehydrogenase and retinoid signaling induces the expansion of human hematopoietic stem cells. Proc Natl Acad Sci USA 103:11707–11712.

Csaszar E, Kirouac DC, Yu M, Wang W, Qiao W, Cooke MP, Boitano AE, Ito C, Zandstra PW. 2012. Rapid expansion of human hematopoietic stem cells by automated control of inhibitory feedback signaling. Cell Stem Cell 10:218–229.

De Felice L, Tatarelli C, Mascolo MG, Gregorj C, Agostini F, Fiorini R, Gelmetti V, Pascale S, Padula F, Petrucci MT, Arcese W, Nervi C. 2005. Histone deacetylase inhibitor valproic acid enhances the cytokine-induced expansion of human hematopoietic stem cells. Cancer Res 65:1505–1513.

Delaney C, Heimfeld S, Brashem-Stein C, Voorhies H, Manger RL, Bernstein ID. 2010. Notch-mediated expansion of human cord blood progenitor cells capable of rapid myeloid reconstitution. Nat Med 16:232–236.

de Lima M, McMannis J, Gee A, Komanduri K, Couriel D, Andersson BS, Hosing C, Khouri I, Jones R, Champlin R, Karandish S, Sadeghi T, Peled T, Grynspan F, Daniely Y, Nagler A, Shpall EJ. 2008. Transplantation of ex vivo expanded cord blood cells using the copper chelator tetraethylenepentamine: a phase I/II clinical trial. Bone Marrow Transplant 41:771–778.

Doetschman TC, Eistetter H, Katz M, Schmidt W, Kemler R. 1985. The in vitro development of blastocyst-derived embryonic stem cell lines: formation of visceral yolk sac, blood islands and myocardium. J Embryol Exp Morphol 87:27–45.

Doulatov S, Notta F, Laurenti E, Dick JE. 2012. Hematopoiesis: a human perspective. Cell Stem Cell 10:120–136.

Foudi A, Hochedlinger K, Van Buren D, Schindler JW, Jaenisch R, Carey V, Hock H. 2009. Analysis of histone 2B-GFP retention reveals slowly cycling hematopoietic stem cells. Nat Biotechnol 27:84–90.

Galić Z, Kitchen SG, Kacena A, Subramanian A, Burke B, Cortado R, Zack JA. 2006. T lineage differentiation from human embryonic stem cells. Proc Natl Acad Sci USA 103:11742–11747.

Galić Z, Kitchen SG, Subramanian A, Bristol G, Marsden MD, Balamurugan A, Kacena A, Yang O, Zack JA. 2009. Generation of T lineage cells from human embryonic stem cells in a feeder free system. Stem Cells 27:100–107.

Gaur M, Kamata T, Wang S, Moran B, Shattil SJ, Leavitt AD. 2006. Megakaryocytes derived from human embryonic stem cells: a genetically tractable system to study megakaryocytopoiesis and integrin function. J Thromb Haemost 4:436–442.

Goessling W, Allen RS, Guan X, Jin P, Uchida N, Dovey M, Harris JM, Metzger ME, Bonifacino AC, Stroncek D, Stegner J, Armant M, Schlaeger T, Tisdale JF, Zon LI, Donahue RE, North TE. 2011.

Prostaglandin E2 enhances human cord blood stem cell xenotransplants and shows long-term safety in preclinical nonhuman primate transplant models. Cell Stem Cell 8:445–458.

Himburg HA, Muramoto GG, Daher P, Meadows SK, Russell JL, Doan P, Chi JT, Salter AB, Lento WE, Reya T, Chao NJ, Chute JP. 2010. Pleiotrophin regulates the expansion and regeneration of hematopoietic stem cells. Nat Med 16:475–482.

Hiroyama T, Miharada K, Aoki N, Fujioka T, Sudo K, Danjo I, Nagasawa T, Nakamura Y. 2006. Long-lasting in vitro hematopoiesis derived from primate embryonic stem cells. Exp Hematol 34: 760–769.

Kaufman DS. 2009. Toward clinical therapies using hematopoietic cells derived from human pluripotent stem cells. Blood 114:3513–3523.

Kaufman DS, Hanson ET, Lewis RL, Auerbach R, Thomson JA. 2001. Hematopoietic colony-forming cells derived from human embryonic stem cells. Proc Natl Acad Sci USA 98:10716–10721.

Kelly SS, Sola CB, de Lima M, Shpall E. 2009. *Ex vivo* expansion of cord blood. Bone Marrow Transplant 44:673–681.

Kissa K, Herbomel P. 2010. Blood stem cells emerge from aortic endothelium by a novel type of cell transition. Nature 464:112–115.

Kiel MJ, Yilmaz OH, Iwashita T, Yilmaz OH, Terhorst C, Morrison SJ. 2005. SLAM family receptors distinguish hematopoietic stem and progenitor cells and reveal endothelial niches for stem cells. Cell. 121:1109–1121.

Kitajima K, Minehata K, Sakimura K, Nakano T, Hara T. 2011. *In vitro* generation of HSC-like cells from murine ESCs/iPSCs by enforced expression of LIM-homeobox transcription factor Lhx2. Blood 117:3748–3758.

Ko KH, Holmes T, Palladinetti P, Song E, Nordon R, O'Brien TA, Dolnikov A. 2011. GSK-3β inhibition promotes engraftment of *ex vivo*-expanded hematopoietic stem cells and modulates gene expression. Stem Cells 29:108–118.

Krause DS, Fackler MJ, Civin CI, May WS. 1996. CD34: structure, biology, and clinical utility. Blood 87:1–13.

Kyba M, Perlingeiro RC, Daley GQ. 2002. HoxB4 confers definitive lymphoid-myeloid engraftment potential on embryonic stem cell and yolk sac hematopoietic progenitors. Cell 109:29–37.

Lancrin C, Sroczynska P, Stephenson C, Allen T, Kouskoff V, Lacaud G. 2009. The haemangioblast generates haematogenic endothelium stage. Nature 457:892–895.

Ledran MH, Krassowska A, Armstrong L, Dimmick I, Renström J, Lang R, Yung S, Santibanez-Coref M, Dzierzak E, Stojkovic M, Oostendorp RA, Forrester L, Lako M. 2008. Efficient hematopoietic differentiation of human embryonic stem cells on stromal cells derived from hematopoietic niches. Cell Stem Cell 3: 85–98.

Li Z, Lan Y, He W, Chen D, Wang J, Zhou F, Wang Y, Sun H, Chen X, Xu C, Li S, Pang Y, Zhang G, Yang L, Zhu L, Fan M, Shang A, Ju Z, Luo L, Ding Y, Guo W, Yuan W, Yang X, Liu B. 2012. Mouse embryonic head as a site for hematopoietic stem cell development. Cell Stem Cell 11:663–675.

Lu SJ, Feng Q, Park JS, Vida L, Lee BS, Strausbauch M, Wettstein PJ, Honig GR, Lanza R. 2008. Biologic properties and enucleation of red blood cells from human embryonic stem cells. Blood 112: 4475–4484.

Lu SJ, Li F, Yin H, Feng Q, Kimbrel EA, Hahm E, Thon JN, Wang W, Italiano JE, Cho J, Lanza R. 2011. Platelets generated from human embryonic stem cells are functional *in vitro* and in the microcirculation of living mice. Cell Res 21:530–545.

Majeti R, Park CY, Weissman IL. 2007. Identification of a hierarchy of multipotent hematopoietic progenitors in human cord blood. Cell Stem Cell 1:635–645.

McCune JM, Namikawa R, Kaneshima H, Shultz LD, Lieberman M, Weissman IL. 1988. The SCID-hu mouse: murine model for the analysis of human hematolymphoid differentiation and function. Science 241:1632–1639.

Mercier FE, Ragu C, Scadden DT. 2011. The bone marrow at the crossroads of blood and immunity. Nat Rev Immunol 12:49–60.

Morrison SJ, Uchida N, Weissman IL. 1995. The biology of hematopoietic stem cells. Annu Rev Cell Dev Biol 11:35–71.

Murray PDF. 1932. The development in vitro of the blood of the early chick embryo. Proc R Soc Lond 11:497–521.

Nakajima-Takagi Y, Osawa M, Oshima M, Takagi H, Miyagi S, Endoh M, Endo TA, Takayama N, Eto K, Toyoda T, Koseki H, Nakauchi H, Iwama A. 2013. Role of SOX17 in hematopoietic development from human embryonic stem cells. Blood 121:447–458.

Nakano T, Kodama H, Honjo T. 1994. Generation of lymphohematopoietic cells from embryonic stem cells in culture. Science 265: 1098–1101.

Namikawa R, Weilbaecher KN, Kaneshima H, Yee EJ, McCune JM. 1990. Long-term human hematopoiesis in the SCID-hu mouse. J Exp Med 172:1055–1063.

Narayan AD, Chase JL, Lewis RL, Tian X, Kaufman DS, Thomson JA, Zanjani ED. 2006. Human embryonic stem cell-derived hematopoietic cells are capable of engrafting primary as well as secondary fetal sheep recipients. Blood 107:2180–2183.

Nishino T, Miyaji K, Ishiwata N, Arai K, Yui M, Asai Y, Nakauchi H, Iwama A. 2009. *Ex vivo* expansion of human hematopoietic stem cells by a small-molecule agonist of c-MPL. Exp Hematol 37: 1364–1377.

Nishino T, Osawa M, Iwama A. 2012. New approaches to expand hematopoietic stem and progenitor cells. Expert Opin Biol Ther 12:743–756.

Nishino T, Wang C, Mochizuki-Kashio M, Osawa M, Nakauchi H, Iwama A. 2011. *Ex vivo* expansion of human hematopoietic stem cells by garcinol, a potent inhibitor of histone acetyltransferase. PLoS One 6:e24298.

North TE, de Bruijn MF, Stacy T, Talebian L, Lind E, Robin C, Binder M, Dzierzak E, Speck NA. 2002. Runx1 expression marks long-term repopulating hematopoietic stem cells in the midgestation mouse embryo. Immunity 16:661–672.

North TE, Gu TL, Stacy T, Wang Q, Howard L, Binder M, Marín-Padilla M, Speck NA. 1999. Cbfa2 is required for the formation of intra-aortic hematopoietic clusters. Development 126:2563–2575.

Notta F, Doulatov S, Laurenti E, Poeppl A, Jurisica I, Dick JE. 2011. Isolation of single human hematopoietic stem cells capable of long-term multilineage engraftment. Science 333:218–221.

Olivier EN, Qiu C, Velho M, Hirsch RE, Bouhassira EE. 2006. Large-scale production of embryonic red blood cells from human embryonic stem cells. Exp Hematol 34:1635–1642.

Osawa M, Hanada K, Hamada H, Nakauchi H. 1996. Long-term lymphohematopoietic reconstitution by a single CD34-low/negative hematopoietic stem cell. Science 273:242–245.

Palis J, Robertson S, Kennedy M, Wall C, Keller G. 1999. Development of erythroid and myeloid progenitors in the yolk sac and embryo proper of the mouse. Development 126:5073–5084.

Peled T, Landau E, Mandel J, Glukhman E, Goudsmid NR, Nagler A, Fibach E. 2004. Linear polyamine copper chelator tetraethylenepentamine augments long-term *ex vivo* expansion of cord blood-derived CD34+ cells and increases their engraftment potential in NOD/SCID mice. Exp Hematol 32:547–555.

Peled T, Shoham H, Aschengrau D, Yackoubov D, Frei G, Rosenheimer G N, Lerrer B, Cohen HY, Nagler A, Fibach E, Peled A. 2012. Nicotinamide, a SIRT1 inhibitor, inhibits differentiation and facilitates expansion of hematopoietic progenitor cells with enhanced bone marrow homing and engraftment. Exp Hematol 40:342–355.

Peschle C, Mavilio F, Carè A, Migliaccio G, Migliaccio AR, Salvo G, Samoggia P, Petti S, Guerriero R, Marinucci M, Lazzaro D, Russo G, Mastroberardino G. 1985. Haemoglobin switching in human embryos: asynchrony of $\zeta \rightarrow \alpha$ and $\varepsilon \rightarrow \gamma$-globin switches in primitive and definite erythropoietic lineage. Nature 313:235–238.

Qiu C, Hanson E, Olivier E, Inada M, Kaufman DS, Gupta S, Bouhassira EE. 2005. Differentiation of human embryonic stem cells into hematopoietic cells by coculture with human fetal liver cells recapitulates the globin switch that occurs early in development. Exp Hematol 33:1450–1458.

Rocha V, Labopin M, Sanz G, Arcese W, Schwerdtfeger R, Bosi A, Jacobsen N, Ruutu T, de Lima M, Finke J, Frassoni F, Gluckman E; Acute Leukemia Working Party of European Blood and Marrow Transplant Group; Eurocord-Netcord Registry. 2004.

Transplants of umbilical-cord blood or bone marrow from unrelated donors in adults with acute leukemia. N Engl J Med 351: 2276–2285.

Sabin FR. 1920. Studies on the origin of blood vessels and of red corpuscules as seen in the living blastoderm of the chick during the second day of incubation: contributions to embryology. Contrib Embryol 9:213–262.

Sudo K, Ema H, Morita Y, Nakauchi H. 2000. Age-associated characteristics of murine hematopoietic stem cells. J Exp Med 192: 1273–1280.

Suzuki T, Yokoyama Y, Kumano K, Takanashi M, Kozuma S, Takato T, Nakahata T, Nishikawa M, Sakano S, Kurokawa M, Ogawa S, Chiba S. 2006. Highly efficient *ex vivo* expansion of human hematopoietic stem cells using Delta1-Fc chimeric protein. Stem Cells 24:2456–2465.

Takahashi K, Tanabe K, Ohnuki M, Narita M, Ichisaka T, Tomoda K, Yamanaka S. 2007. Induction of pluripotent stem cells from adult human fibroblasts by defined factors. Cell 131:861–872.

Takayama N, Eto K. 2012. Pluripotent stem cells reveal the developmental biology of human megakaryocytes and provide a source of platelets for clinical application. Cell Mol Life Sci 69:3419–3428.

Takayama N, Nishikii H, Usui J, Tsukui H, Sawaguchi A, Hiroyama T, Eto K, Nakauchi H. 2008. Generation of functional platelets from human embryonic stem cells in vitro via ES-sacs, VEGF-promoted structures that concentrate hematopoietic progenitors. Blood 111:5298–5306.

Takayama N, Nishimura S, Nakamura S, Shimizu T, Ohnishi R, Endo H, Yamaguchi T, Otsu M, Nishimura K, Nakanishi M, Sawaguchi A, Nagai R, Takahashi K, Yamanaka S, Nakauchi H, Eto K. 2010. Transient activation of c-MYC expression is critical for efficient platelet generation from human induced pluripotent stem cells. J Exp Med 207:2817–2830.

Thomson JA, Itskovitz-Eldor J, Shapiro SS, Waknitz MA, Swiergiel JJ, Marshall VS, Jones JM. 1998. Embryonic stem cell lines derived from human blastocysts. Science 282:1145–1147.

Tian X, Woll PS, Morris JK, Linehan JL, Kaufman DS. 2006. Hematopoietic engraftment of human embryonic stem cell-derived cells is regulated by recipient innate immunity. Stem Cells 24: 1370–1380.

Timmermans F, Velghe I, Vanwalleghem L, De Smedt M, Van Coppernolle S, Taghon T, Moore HD, Leclercq G, Langerak AW, Kerre T, Plum J, Vandekerckhove B. 2009. Generation of T cells from human embryonic stem cell-derived hematopoietic zones. J Immunol 182:6879–6888.

Togarrati PP, Suknuntha K. 2012. Generation of mature hematopoietic cells from human pluripotent stem cells. Int J Hematol 95: 617–623.

Ueda T, Tsuji K, Yoshino H, Ebihara Y, Yagasaki H, Hisakawa H, Mitsui T, Manabe A, Tanaka R, Kobayashi K, Ito M, Yasukawa K, Nakahata T. 2000. Expansion of human NOD/SCID-repopulating cells by stem cell factor, Flk2/Flt3 ligand, thrombopoietin, IL-6, and soluble IL-6 receptor. J Clin Invest 105:1013–1021.

Vodyanik MA, Bork JA, Thomson JA, 2005. Slukvin II. Human embryonic stem cell-derived CD34+ cells: efficient production in the coculture with OP9 stromal cells and analysis of lymphohematopoietic potential. Blood 105:617–626.

Vogel W, Scheding S, Kanz L, Brugger W. 2000. Clinical applications of CD34(+) peripheral blood progenitor cells (PBPC). Stem Cells 18:87–92.

Wang JC, Doedens M, Dick JE. 1997. Primitive human hematopoietic cells are enriched in cord blood compared with adult bone marrow or mobilized peripheral blood as measured by the quantitative in vivo SCID-repopulating cell assay. Blood 89:3919–3924.

Wang LD, Menendez P, Shojaei F, Li L, Mazurier F, Dick JE, Cerdan C, Levac K, Bhatia M. 2005. Generation of hematopoietic repopulating cells from human embryonic stem cells independent of ectopic *HOXB4* expression. J Exp Med 201:1603–1614.

Wang LD, Wagers AJ. 2011. Dynamic niches in the origination and differentiation of haematopoietic stem cells. Nat Rev Mol Cell Biol 12:643–655.

Weissman IL. 2000. Stem cells: units of development, units of regeneration, and units in evolution. Cell 100:157–168.

Ye Z, Chou BK, Cheng L. 2012. Promise and challenges of human iPSC-based hematologic disease modeling and treatment. Int J Hematol 95:601–609.

Yu J, Vodyanik MA, Smuga-Otto K, Antosiewicz-Bourget J, Frane JL, Tian S, Nie J, Jonsdottir GA, Ruotti V, Stewart R, Slukvin II, Thomson JA. 2007. Induced pluripotent stem cell lines derived from human somatic cells. Science 318:1917–1920.

Zambidis ET, Peault B, Park TS, Bunz F, Civin CI. 2005. Hematopoietic differentiation of human embryonic stem cells progresses through sequential hematoendothelial, primitive, and definitive stages resembling human yolk sac development. Blood 106:860–870.

Zhang CC, Kaba M, Iizuka S, Huynh H, Lodish HF. 2008. Angiopoietin-like 5 and IGFBP2 stimulate ex vivo expansion of human cord blood hematopoietic stem cells as assayed by NOD/SCID transplantation. Blood 111:3415–3423.

Stem Cell Reports
Report
ISSCR
OPEN ACCESS

The TIF1β-HP1 System Maintains Transcriptional Integrity of Hematopoietic Stem Cells

Satoru Miyagi,[1,3] Shuhei Koide,[1,3] Atsunori Saraya,[1,3] George R. Wendt,[1,4] Motohiko Oshima,[1,3] Takaaki Konuma,[1] Satoshi Yamazaki,[5] Makiko Mochizuki-Kashio,[1,3] Yaeko Nakajima-Takagi,[1,3] Changshan Wang,[1,3] Tetsuhiro Chiba,[2] Issay Kitabayashi,[6] Hiromitsu Nakauchi,[5] and Atsushi Iwama[1,3,*]

[1]Department of Cellular and Molecular Medicine, Graduate School of Medicine, Chiba University, Chiba 260-8670, Japan
[2]Department of Medicine and Clinical Oncology, Graduate School of Medicine, Chiba University, Chiba 260-8670, Japan
[3]JST, CREST, Sanbancho, Chiyoda-ku, Tokyo 102-0075, Japan
[4]ITO Foundation for International Education Exchange, Shinjuku 160-0023, Japan
[5]Division of Stem Cell Therapy, Center for Stem Cell Biology and Regenerative Medicine, Institute of Medical Science, University of Tokyo, Tokyo 108-8639, Japan
[6]Division of Hematological Malignancy, National Cancer Center Research Institute, Tokyo 104-0045, Japan
*Correspondence: aiwama@faculty.chiba-u.jp
http://dx.doi.org/10.1016/j.stemcr.2013.12.008

SUMMARY

TIF1β is a transcriptional corepressor that recruits repressive chromatin modifiers to target genes. Its biological function and physiological targets in somatic stem cells remain largely unknown. Here, we show that TIF1β is essential for the maintenance of hematopoietic stem cells (HSCs). Deletion of *Tif1b* in mice induced active cycling and apoptosis of HSCs and promoted egression of HSCs from the bone marrow, leading to rapid depletion of HSCs. Strikingly, *Tif1b*-deficient HSCs showed a strong trend of ectopic expression of nonhematopoietic genes. Levels of heterochromatin protein 1 (HP1α, β and γ) proteins, which form a complex with TIF1β, were significantly reduced in the absence of TIF1β and depletion of HP1 recapitulated a part of the phenotypes of *Tif1b*-deficient HSCs. These results demonstrate that the TIF1β-HP1 system functions as a critical repressive machinery that targets genes not normally activated in the hematopoietic compartment, thereby maintaining the transcriptional signature specific to HSCs.

INTRODUCTION

During hematopoiesis, hematopoietic stem cells (HSCs) activate specific sets of genes and silence others. Transcription factors fulfill an obvious role in this process. At the same time, chromatin modifiers regulate the accessibility of transcription factors to *cis* elements by establishing regions of chromatin that are either permissive or repressive to transcription. These epigenetic transcriptional regulations are crucial for the maintenance of multipotency in stem cells (Sauvageau and Sauvageau, 2010; Sashida and Iwama, 2012). Polycomb group (PcG) proteins, which establish a reversible silencing state through repressive histone modifications, maintain multipotency of HSCs by keeping hematopoietic developmental regulator genes poised for activation via bivalent histone domains (Oguro et al., 2010). However, the mechanisms by which nonhematopoietic genes, which should never be activated in the hematopoietic cell lineage, are transcriptionally repressed remain to be elucidated.

TIF1β (also called KAP1 or TRIM28) is a transcriptional corepressor that associates with hundreds of Kruppel-associated box domain-zinc finger proteins (KRAB-ZFPs) that bind DNA in a sequence-specific fashion. TIF1β acts as a scaffold for a multimolecular complex that silences transcription through the formation of heterochromatin by recruiting the histone methyltransferase SETDB1, heterochromatin protein 1 (HP1), or the NuRD-histone deacetylase complex (Nielsen et al., 1999; Schultz et al., 2001, 2002). The KRAB/KAP1 system plays a critical role in the control of endogenous retroviruses during development (Rowe et al., 2010, 2013) but also regulates multiple aspects of mammalian physiology. In hematopoiesis, it functions in erythropoiesis and in the prevention of autoinflammatory T cell development (Chikuma et al., 2012; Barde et al., 2013).

In this study, we demonstrate an essential role for the TIF1β/HP1 system in the maintenance of HSCs and implicate this system in the establishment of transcriptional signature of HSCs by keeping nonhematopoietic genes transcriptionally silent.

RESULTS AND DISCUSSION

Deletion of *Tif1b* Severely Compromises HSC Function in the Fetal Liver

Tif1b-deficient mice show early developmental defects and die by embryonic day 7.5 (E7.5) (Cammas et al., 2000). To delineate function of TIF1β in HSCs, we conditionally deleted *Tif1b* by crossing *Tif1b*$^{fl/fl}$ mice with *Tie2-Cre* mice, which specifically express *Cre* in hematopoietic and endothelial cells (*Tie2-Cre;Tif1b*$^{fl/fl}$). We confirmed efficient

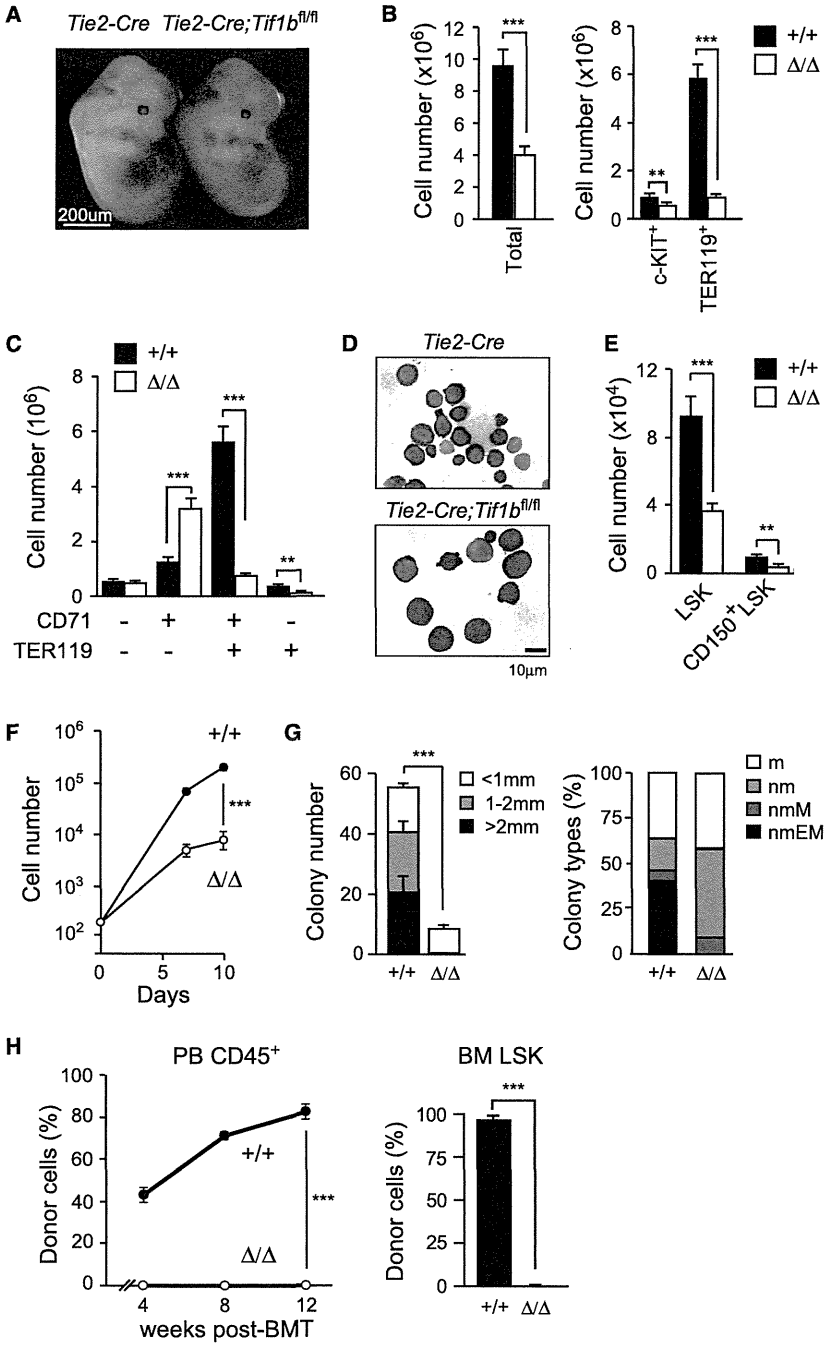

Figure 1. *Tie2-Cre;Tif1b*$^{fl/fl}$ Embryos Die at Midgestation

(A) Appearance of *Tie2-Cre* (*Tif1b*$^{+/+}$) and *Tie2-Cre;Tif1b*$^{fl/fl}$ (*Tif1b*$^{\Delta/\Delta}$) embryos at E13.5.

(B) Absolute numbers of whole fetal liver cells, c-KIT$^+$ progenitors, and TER119$^+$ erythroblasts at E13.5. The data are shown as mean ± SEM (*Tie2-Cre*, n = 16; *Tie2-Cre;Tif1b*$^{fl/fl}$, n = 17).

(C) Absolute numbers of erythroid cells at different stages defined by CD71 and TER119 expression in fetal livers at E13.5. The data are shown as mean ± SEM (*Tie2-Cre*, n = 16; *Tie2-Cre;Tif1b*$^{fl/fl}$, n = 17).

(D) Morphology of *Tif1b*$^{+/+}$ and *Tif1b*$^{\Delta/\Delta}$ fetal liver hematopoietic cells from E13.5 embryos stained with May-Grünwald-Giemsa solution.

(E) Absolute cell numbers of LSK and CD150$^+$LSK cells in the fetal liver at E13.5. The data are shown as mean ± SEM (*Tie2-Cre*, n = 23; *Tie2-Cre;Tif1b*$^{fl/fl}$, n = 21).

(F) Growth of *Tif1b*$^{+/+}$ and *Tif1b*$^{\Delta/\Delta}$ LSK cells from E13.5 fetal livers in liquid culture in the presence of 50 ng/ml of SCF and TPO. The data are shown as mean ± SEM for triplicate cultures.

(G) Colony-forming assays with *Tif1b*$^{+/+}$ and *Tif1b*$^{\Delta/\Delta}$ fetal liver cells. Left panel shows the absolute number of colonies with the indicated size per 20,000 fetal liver cells. The data are shown as mean ± SEM for triplicate cultures. Right panel shows the proportion of colony types defined by the composition of colony-forming cells (n, neutrophil; m, macrophage; E, erythroblast; M, megakaryocyte).

(H) Competitive repopulating assays. A total of 2 × 10^5 *Tif1b*$^{+/+}$ and *Tif1b*$^{\Delta/\Delta}$ fetal liver cells from E13.5 embryos (CD45.2) mixed with the same number of competitor BM cells (CD45.1) were transplanted into CD45.1 recipients. Chimerism of donor-derived CD45.2$^+$ cells in the PB is shown in the left panel. Donor chimerism in the BM LSK cells at 12 weeks posttransplantation is shown in the right panel. The data are shown as mean ± SEM (n = 6). *p < 0.05; **p < 0.005; ***p < 0.0005.

deletion of *Tif1b* in fetal liver lineage-marker (Lin)$^-$c-KIT$^+$ hematopoietic progenitor cells from *Tie2-Cre;Tif1b* mice by western blot and immunocytochemical analyses in Lin$^-$c-KIT$^+$SCA-1$^+$ (LSK) hematopoietic stem and progenitor cells (HSPCs) (Figures S1A and S1B available online). *Tie2-Cre;Tif1b*$^{fl/fl}$ embryos were recovered at nearly the expected Mendelian ratio at E13.5, but about 28% (58 out of 207 *Tie2-Cre;Tif1b*$^{fl/fl}$ embryos) were already dead and no mutant embryos were born alive (data not shown). *Tie2-Cre;Tif1b*$^{fl/fl}$ embryos were pale and their fetal livers were significantly smaller than those of the littermate controls (Figures 1A and 1B). Flow cytometric analyses